JPRS-UST-94-015
5 AUGUST 1994

FOREIGN BROADCAST INFORMATION SERVICE

JPRS Report

Science & Technology

Central Eurasia

NUCLEAR DEVELOPMENTS IN CIS

JPRS-UST-94-015
5 AUGUST 1994

SCIENCE & TECHNOLOGY

CENTRAL EURASIA

NUCLEAR DEVELOPMENTS IN CIS

CONTENTS

Operational Reliability Analysis of Generating Unit With BN-600 During 1980-1993

947F0148A Moscow ATOMNAYA ENERGIYA in Russian Vol 76 No 3, Mar 94 pp 167-171

[Article by N.N. Oshkanov, A.G. Sheynkman, and P.P. Govorov, Beloyarskiy Nuclear Power Plant; UDC 621.039.526:621.311.22]

[Text] The third generating unit of the Beloyarskiy NPP with a BN-600 reactor was commissioned in April 1980 and has operated successfully for 14 years. During this period, the following goals formulated during its development were accomplished: safe and reliable operation of the sodium reactor with a high unit power, extended safe life tests of large hardware operating in a sodium environment, validation of the sodium technology and procedures of replacing and repairing the equipment, and verification and improvement of the operating conditions.

The operating and testing experience generally confirms the validity of the design decisions made yet at the same time identifies the drawbacks which call for upgrading and redesigning equipment elements (main circulating pump (GTsN), steam generators, sodium valves, etc.). Certain unit operating conditions were also corrected: the loop activation conditions and steam generator operation without one of the eight sections; the unit shut-down condition with low-speed emergency protection operation was completely eliminated.

General reliability characteristics. The generating unit operating history can be tentatively divided into two periods: from April 1980 through September 1981--verification by a stage-by-stage power increase from 30 to 80% and from October 1981 through December 1993--operation with commercial electric power generation.

As of 31 Dec 93, the total power generation reached 49.69 billion kWh with a total length of power operation of ~91,000 h, a mean gross efficiency, net efficiency, and housekeeping power consumption of 41, 38, and 7%, respectively. Prior to 1987, the reload cycle microcampaign was equal to 100 days, and after the transition to an upgraded core after the 19th life cycle in June 1987, it increased to 165 days.

The installed capacity utilization was equal to 68.74%. Starting with 1983, the mean installed capacity utilization coefficient was equal to approximately 73-75%, and in 1992, it reached 83.5% for the first time. This decrease in the installed capacity utilization was due to the power unit shutdown for scheduled maintenance (21.4%), primary equipment failures (5.3%), and power pickup (4.6%). The technical utilization factor during the same period amounted to 75.7% whereby during 7.6% of the time, the power unit operated with three loops and during 5.1% of the time--with two loops. Time under utilization due to scheduled preventive maintenance was 22.1% and due to the power generation unit recovery following total failures--2.2%.

During its 14 years of operation, the generating unit availability factor was 97.2%. The power unit unavailability was largely due to the fuel element assembly (TVS) recharging necessitated by the fuel element leakage (1.3%), generating unit power down for connecting the third loop after its repairs (0.6%), reactivity control system (SKUZ) failures (0.3%), and operating and maintenance personnel errors (0.2% each). Altogether, normal generating unit operation was violated 97 times due to unscheduled complete or partial decreases in the generating unit power (without taking into account the violations occurring during the generating unit start-up prior to the turbogenerator connection to the network) [1, 2].

In 27 cases, normal generating unit operation violations due to equipment and system failures were accompanied by a generating unit shutdown, and in 21 of these cases, high-speed emergency protection operated (in six cases, control rods were dropped by the operator), while in the remaining 70 cases, generating unit output dropped and in 56 cases, this was accompanied by a loop disconnection (initiated by the operator in 24 of these cases). Moreover, the generating unit downtime amounted to ~2,500 h and operation at a decreased power--to ~7,600 h.

Disruptions in the normal generating unit operating conditions can be divided into two groups: due to staff errors and due to basic equipment failures. Normal operation disruptions due to personnel errors amounted to 20.6% (of this, 12.4% were due to operating personnel error and 8.2%--due to maintenance personnel), while 79.4% are due to disruptions resulting from equipment failures.

Equipment. The principal reasons of the equipment and generating unit system failures are as follows, in %: structural and configurational shortcomings (36.1), manufacturing defects (19.6), poor repairs (15.5), and assembly and adjustment flaws (4.1) (Fig. 1). The largest number of normal generating unit operation disruptions due to equipment failures was due to reactivity control system failures (19.6% of the total number of disruptions), failures of the third loop and water circulation system equipment (13.4%), failures of the primary and secondary loop main circulating pumps (11.4%), electrical equipment failures (11.3%) (Table 1), and fuel element depressurization in the fuel element assembly (10.3%) (Fig. 2). During the entire generating unit operating period, third circuit and water circulation system equipment failures were required to decrease the generating unit power in 13 cases.

There were a total of 19 normal generating unit operation disruptions due to reactivity control system failures. Of these, eight normal operation disruptions were caused by false protection system operations, i.e., without the need for their operation, and in four cases, protection system operation was excessive when a false signal requiring its operation was generated. Reactivity control system failures were largely due to design and configurational shortcomings (11) and manufacturing defects (7) which were resolved by improving the signal conditioning and emergency protection relay sequencing systems.

Electrical equipment failures were largely associated with turbogenerators (seven out of the 11 electrical equipment failures) and with the need to shut them down in order to detect and fix hydrogen leaks. Vertical centrifugal pumps with a base hydrostatic thrust bearing were used as the main circulation pumps in the sodium loops. During the field development of the generating unit prior to March 1981, GTsN-1 and -2 operated without noticeable problems, yet when it was

necessary once again to increase the rotation speed in order to increase the generating unit power, the pump shaft linkages with the electric motor began to fail [3].

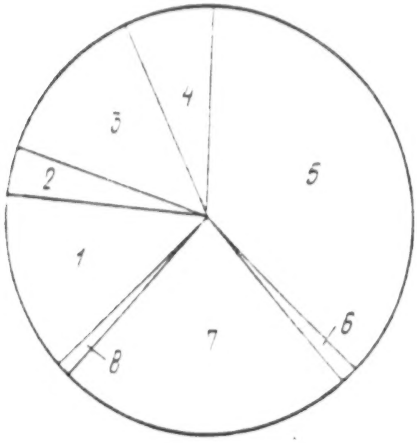

Fig. 1. Distribution of the generating unit power decreases due to poor maintenance and repairs--15.5% (1), assembly and adjustment flaws--4.1% (2), operating and maintenance personnel errors--12.4% (3) and 8.2% (4), respectively, manufacturing flaws--19.6% (5), metal defects--3.1% (6), design and configuration shortcomings--36.1% (7), and primary loop coolant impurities--1% (8).

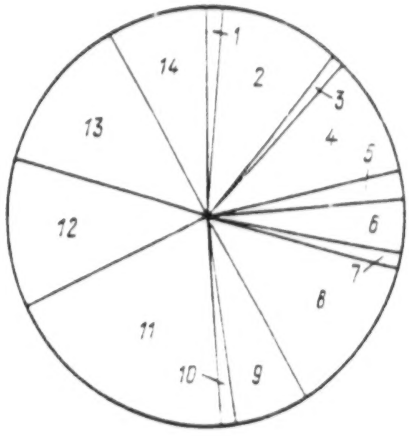

Fig 2. Distribution in the number of generating unit power decreases due to equipment failures and personnel errors (in %): 1--Reactor (1); 2--Fuel element assembly (10.3); 3--Primary loop equipment (1); 4, 5--Main circulating pump of the first (9.3) and second loop (2.1); 6--Steam generator (4.2); 7, 8--Second (1) and third loop equipment (12.4), respectively; 9--Turbine (6.2); 10 and 11--Circulating water supply system equipment (1) and reactivity control system (19.6), respectively; 12--Electrical equipment (11.3); 13, 14--Operating (12.4) and maintenance personnel errors (8.2).

Table 1. Equipment, third loop pipeline, and circulating water supply system failures

Equipment	Failure Cause	Number
Valves	Leakage	4
	Jamming	2
Mechanical filter	Leakage	2
Turbine receiver	Leakage	1
Turbine seal steam cooler	Leakage	1
Pipelines	Flaw	2
	Rupture	1

Furthermore, elevated GTsN-1 vibration was observed in 1982-1984, cracks appeared in the shafts, half-couplings in the pump shaft clutch with the electric motor rotor were damaged, and unreliable electric drive operation was observed. The half-coupling and shaft damage was due to the torsional vibration resonance in the working rotation frequency band and the merger of the output power fluctuations of the electric drive with the natural frequency of the shaft torsional vibrations. The shafts and half-couplings were upgraded in order to ensure normal GTsN-1 performance, and the operating GTsN-1 rotation frequency was set outside the resonance range, while the electric motor was switched to an uncontrolled operating mode after the generating unit reached more than 85% of rated power. After that, starting with the 15th microcampaign (December 1985), no GTsN-1 failures leading to normal performance disruptions have been observed.

Sectioned-modular steam generators with straight tubes are used in the generating unit; each consists of eight sections with three modules in each--an evaporator, a steam superheater, and a reheater. Experience demonstrates that these are characterized by a high operational reliability. The possibility of steam generator operation at a rated power with 7 sections was verified experimentally [4, 5]. As a result, in 12 failures caused by interloop leakage, it was necessary to disconnect the loop in only three cases and shut down the unit only once.

An investigation into the steam generator module damage causes [4] reveals that the most likely causes of the lack of pressurization between the loop and in the modules are the manufacturing defects not detected during tests at the manufacturing plant using conventional inspection methods. During the past 14 years, the steam generator reliability has been increased; for this purpose, prestart and chemical washing procedures have been developed, structural flaws in the principal sodium valves have been eliminated, and the steam superheater module lid sealing units have been upgraded.

Reactor core. The BN-600 design incorporates a high energy stress in the reactor core and a maximum linear load of 500 W/cm with a fuel element cladding temperature of 710°C at a specific power of 810 kW/l. Yet the structural materials and the design solution involving rearrangement and rotation of the peripheral assemblies in the cases of overloads could not ensure attainment of the maximum fuel burn-up of 9.7% of heavy atoms stipulated by the design. During the operating life, 119 fuel element assemblies with depressurized fuel elements across the gas and 80 depressurized elements across the fuel were detected; their detection and recharging called for six unscheduled generating unit discharging operations and three instances of lowering its power. A 7% heavy atom limit on the maximum burn-up did not prevent the fuel element cladding depressurization which continued up to the 18th microcampaign (January 1987).

In order to increase the performance reliability and raise the permissible fuel burn-up, the core was upgraded in 1986-1987. The maximum linear load was decreased to 480 W/cm by increasing the core height from 750 to 1,000 mm, a transition from two to three enrichment zones was executed (17, 21, and 26% for ^{235}U), new structural materials were used in the jacket (cold strained austenitic steel 08Kh16N11M3T and ferritic martensitic steel EP-450) and in fuel element cladding (austenitic class steel with cold straining EP-172 and ChS-68), while the fuel assembly operating procedures were revised. As a result of these measures, there have been no normal performance disruptions of the generating unit due to the fuel element assembly cladding depres-

surization since the 18th microcampaign, and the maximum fuel burn-up reached 10% of heavy atoms.

Operating personnel. The operating personnel at the generating unit is staffed with six shifts with 30 persons in each. During the period under study, 12 normal generating unit operation disruptions have occurred due to operating personnel errors. Most of the errors (six out of 12) occurred during the initial operating period (1980-1981) of which five happened during the first microcampaign; three operating personnel errors can be classified as instantaneous, i.e., resulting in a power unit output decrease immediately after the incorrect actions were taken: On 26 Nov 83 (the 9th microcampaign), the generating was shut down due to the excessive operation of the GTsN-1 rpm overspeed protection in the fourth loop due to a short circuit caused by incorrect personnel actions while measuring the blinker voltage; on 26 Feb 85 (13th microcampaign), the loop was deactivate due to the turbogenerator power-down as a result of erroneous disconnection of the generator excitation when it was being switched to standby excitation; and on 28 Dec 87 (20th microcampaign), the loop was deactivated because the turbogenerator was shut down by the protection system as a result of an oil level drop in the damper oil tank because the gates were closed erroneously in the oil delivery line to the generator seal bearings while the oil filters were being changed.

The mean time between operating personnel errors (T), the operating personnel error rate (e), and probability of error-free operating personnel performance (P) during a given time interval were defined for the operating personnel [6]. The time interval was selected to be equal to the duration of one microcampaign (165 days). Based on the low number of errors, these indicators were evaluated by a nonparametric method using the procedure described in [7] (Table 2).

Table 2. Disruptions in normal generating unit performance due to operating personnel errors (12 cases between 8 Apr 80 and 31 Dec 93)

Reliability Indicator	Point Estimate	Confidence estimate at q = 0.8	
		Lower bound	Upper bound
e, 1/h	$4.39 \cdot 10^{-6}$	$3.30 \cdot 10^{-6}$	$5.82 \cdot 10^{-6}$
T m h	$228 \cdot 10^{3}$	$172 \cdot 10^{3}$	$303 \cdot 10^{3}$
P	0.983	0.987	0.977

Summary. The high quality of the design and the modifications of the principal basic equipment and system units carried out during the initial performance phase (GTsN-1, steam generators, and reactivity control system) made it possible to ensure reliable generating unit operation. The following comprehensive reliability indicators have been achieved, in %: an installed capacity utilization factor, technical utilization factor, and availability factor of 68.7, 75.7, and 97.2, respectively. A maximum capacity utilization factor of 77% was attained in 1988.

The normal generating unit performance disruptions due to equipment failures and personnel errors did not lead to an exceedance of the safe operation limits established by the design. Most of the disruptions (~75%) fall within 1980-1986, while the mean number of violations is approxi-

mately seven cases per year; there have been four cases per year between 1987 and 1990. In recent years (1988-1993), normal generating unit operation violations (21 cases) were largely due to turbogenerator failures (five cases) and third loop equipment failures (three cases).

Bibliography

1. OPB-88 Pravila i normy v atomnoy energetike (OPB-88 Nuclear power industry rules and standards. General premises of nuclear power plant safety assurance). Moscow: Energoatomizdat, 1990).

2. N.N. Oshkanov, A.G. Sheynkman, P.P. Govorov. Generating unit with BN-600 fast sodium reactor: Reliability assessment during the 1980-1990 operating period. Preprint of the Urals Department of Russia's Academy of Sciences, Seriya Yadernaya energetika. Yekaterinburg, 1992.

3. O.M. Sarayev, N.N. Oshkanov, A.G. Sheynkman. BN-600 generating unit: Operating experience. In: Teplofizika yadernykh energeticheskikh ustanovok (Thermal physics of nuclear power plants). Issue 5. Sverdlovsk, Urals Polytechnic Institute, 1987, pp. 145-151.

4. V.V. Stekolnikov, B.I. Lukasevich, V.F. Titov, *et al.* Sodium-water steam gnerator operating experience in the USSR and development outlook. In: Bystryye reaktory (Fast reactors. Experience and development trends). Proceedings of the International Symposium, Lyon, France, 1985. Vol. 2. IAEA Report No. IAEA-SM-284/34, 1986.

5. A.G. Sheynkman, A.I. Beltyukov, V.V. Vylomov, *et al.* Performance assessment of the thermal and hydraulic properties of BN-600 generating unit steam generators. *Teploenergetika* No. 12, 1989, pp. 15-18.

6. B. Dillon, Ch. Singh. Engineering methods of system reliability assurance. Moscow: Mir, 1984.

7. RD50-690-89. Nadezhnost v tekhnike (Reliability in Engineering. Methods of assessing reliability indicators on the basis of experimental findings. Procedures manual). Moscow: USSR State Committee on Quality Control Management and Sttandards, 1990.

Drop in Demand for Natural Uranium

947F0148B Moscow ATOMNAYA ENERGIYA in Russian Vol 76 No 3, Mar 94 pp 175-182

[Article by B.V. Nikipelov, Russian Federal Ministry of Nuclear Power Industry; UDC 546.791.-338]

[Text] The dismantling of the state monopoly and liberalization of the foreign trade regime in Russia and CIS increased these countries' supply of goods to the world market. There was excess supply of many goods in the world market even before, yet access of CIS goods to the market has boosted this supply even further.

The competitiveness of such materials, goods, and to a lesser extent, machines whose quality indicators meet world standards (aluminum, other nonferrous and rare metals, including uranium, ferrous metals, fertilizers, armaments, etc.) and which have a low cost of production in the West is high. In some cases, this aggravated the already existing trend toward depressing the prices and led to countermeasures by foreign companies, some with government assistance. The latter adopted protectionist measures against the new market participants instead of taking steps against the unjustified drop in prices, which is illogical and inconsistent.

The purpose of this article is to use the example of the uranium market to demonstrate that the reason for the existing situation is not only the fault of CIS enterprises and companies but also a consequence of the respective government decisions to deregulate market relations for such strategic goods and to show that regulatory measures are necessary by means of limiting production and prices on the basis of multilateral intergovernmental agreements and general strategic concepts of various production trends. The purpose of this article is not to predict the development of the uranium market and its production and demand but to present an option of the nuclear fuel cycle objective and strategy of most nuclear powers during 1994-2020--to minimize uranium mining--including the maximum resource conservation--and, most importantly, sales of the stocks of weapons-grade uranium and later--of plutonium.

Uranium production, stocks, market, and outlook. Let us examine certain data on the natural uranium production, demand, and market in the world. The demand, supply, and forecast for the year 2000 made by one of the leading uranium business companies in Western Europe are shown in Fig. 1 [1].

The status of uranium production, demand, and market is carefully analyzed by the *Nuexco review* journal. Data on the uranium production and demand, including such Eastern Bloc countries as Bulgaria, China, the Czech Republic, the former GDR, Hungary, Kazakhstan, Kyrgyzstan, Poland, Romania, Russia, Tajikistan, Ukraine, and Uzbekistan are published in its last issues for

1993. When data were not available, journal estimates were used (Fig. 2). Following an anti-dumping investigation in the United States in 1992, customs tariffs were introduced on uranium imports from the CIS, primarily from Russia, which virtually halted uranium trade between Russia and the United States. Nevertheless, new articles appeared in 1993 which accused Russia of all uranium market misfortunes. The situation which developed in 1993 and the outlook for 1994 are rather favorable in the opinion of the International Uranium Institute (London). Supply barely meets 66% of demand. The shortfall amounting to 22-25 thousand tons is made up by using uranium from the reserves. Although uranium production is dropping in the CIS, some 50-400 thousand are in storage, which may fully meet world demand for 1-10 years, as noted in the article [2]. It was stated at the Moscow meeting-seminar on "Nuclear Safety in the Former Soviet Union" held in January 1993 and attended by representatives from the European Energy Fund, European Parliament, European Community Commission, Russia's Atomic Ministry, and the "Kurchatov Institute" Scientific Research Center that the European Community is expecting that Russia would curtail uranium exports to the European market in exchange for expert studies of nuclear power plant safety in Russia and deliveries of emergency systems to NPPs [3].

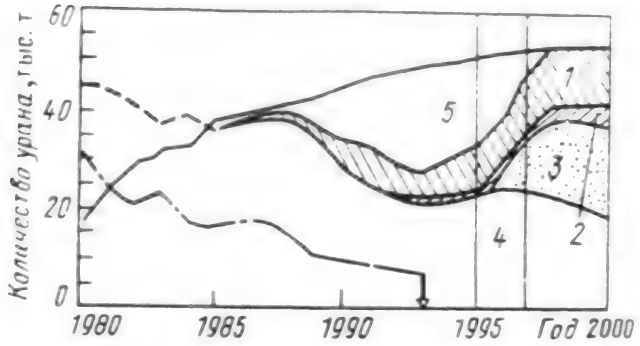

Fig. 1. Supply and demand balance in Western countries: 1--CIS and PRC import; 2--Reprocessing; 3--New production; 4--Price jump; 5--Plant access stock decrease; (---)--Current production; (—)--Demand; (-.-.-)--Wholesale price; Y-axis--Quantity of uranium in thousand tons

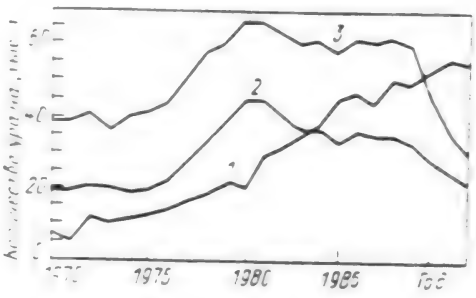

Fig. 2. Uranium production and demand in the world: 1--Annual demand; 2--Annual production; 3--Annual demand; Y-axis--Quantity of uranium, in thousand tons

For an objective assessment and conclusions drawn from the causes of today's uranium market conditions, let us examine the analyses which were made in 1993 [4]. One can see from examining Fig. 3 that following a stable and low price level for 1973, prices began to rise sharply in 1974-1976 and increased by approximately 2.5 times. This increase, in turn, was caused by a dropping increase in warehouse stocks in 1970-1974 (although some tend to attribute it to the oil crisis).

The uranium price increase in 1974 was immediately followed by an increase in uranium production which, naturally, was slower than the price increase. Due to a considerable increase in the warehouse stocks, short-term market prices began to drop sharply in 1980 following a short period of stability in 1978-1979. Although the ensuing sharp slowdown in the warehouse stock

increase did dampen the price drop somewhat, it did not arrest it. And all this occurred in the world market without any CIS natural uranium being present there.

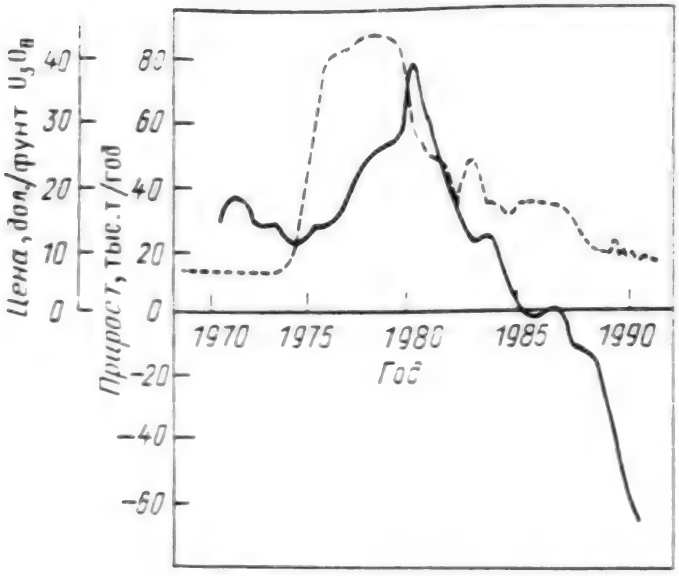

Fig. 3. Uranium price fluctuation in the short-term market (---) and an increase in warehouse capacity (—) (without Russia and CIS): Left Y-axis, U_3O_8 price, dollar pound; Right Y-axis--Annual increase, thousand t/year.

Utilization of the warehouse stocks, albeit on a small scale, began in the West in 1986 and is continuing today but on a greater scale. So the emergence of USSR on the world market in 1989 also reflected its natural desire to decrease the warehouse stocks and excess production capacities.

The following conclusions can be drawn from analyzing Figs. 1-3 which characterize supply and demand in the world uranium market:

the decline in output and a drop in the stock market prices can be attributed to a considerable overproduction of uranium in the world, primarily in the West, and later in the Eastern Bloc countries;

hopes that natural uranium production may increase from the present level either in 1995 or in 1997 are groundless as are the hopes of a market price jump since an increase in uranium prices is possible only in the framework of international agreements. Moreover, hopes for new production and the anticipated price jump emanate from the expectation of a sharp decline and termination of uranium deliveries from Western warehouse stocks in 1995. But why cannot one take into account warehouse stocks in the CIS as well as the enriched uranium market resulting from the dismantling of nuclear weapons, both in Russia and the United States?

Yet the most important is to answer the question: Why is an increase in the quantity of mined uranium a benefit and strategically correct policy? This is profitable for companies which mine uranium, but is it profitable as a whole for the nuclear fuel cycle, nuclear power industry, and the society at large? The answer to this question will not reflect the official position of any

department but present the opinion of one of the experts as well as some specialists in the nuclear fuel cycle.

Although it is obvious to the author of this article that there is no reason to develop new uranium mining production in 1995-2000, what is fundamental is to determine the strategy for the period of 2015-2020. In this analysis, it would be desirable to give more attention to the environmental rather than economic and technical issues, yet the latter two cannot be underestimated. From the environmental viewpoint, the advantage of the nuclear power industry is that a lot less fuel (uranium) and the accompanying raw material is expended per unit of energy released than in traditional utilization of coal, oil, and gas. This means that the mineral resources suffer less loss, fewer rock spoil heaps and gangue have to be reprocessed, there are fewer sludge fields and discharges, etc. According to the data from the International Uranium Institute, today a high-power reactor consumes 150 t of natural uranium per year which is an equivalent of 2 million t of coal or 10 million barrels of oil [5], i.e., its mass is 6.5 thousand times less than that of coal. According to some analyses, an increase in the burn-up fraction to 60 MW·day/kg can increase this ratio: 1 t of uranium is equivalent to 80 thousand tons of equivalent fuel.

A nuclear power industry development forecast to the year 2010 prepared by the IAEA (MAGA-TE) [6] estimates a minimum increase in the total NPP capacity compared to 1990 as 1.4 times and the maximum as 1.8 times. Assuming that the fuel utilization factor remains unchanged, the demand for natural uranium will increase. (This is probably used as the basis of the predicted increase in uranium consumption shown in Fig. 1). Yet many companies, e.g., FdF in France, are planning on implementing fuel with a greater burn-up fraction starting with 1995. It has been demonstrated in the analyses by our country's experts that given an increase in the fuel burn-up fraction of VVER-1000 from 30 to 60 MW·day/kg, uranium demand decreases by 1.87 times.

It is indicated in [7] that when in the future conversion ratios increase to 0.7-0.8 in the case of, e.g., closely spaced lattices, natural uranium consumption may decrease by approximately two-fold. Consequently, implementation of such developments may compensate for an increase in the total nuclear power plant capacity not only by 2010 but already by 2005-2015 and maybe even earlier by decreasing the total natural uranium consumption by 5-30% compared to the 2000 level. Thus, in analyzing natural uranium balance in 2000-2020, one can assume that the level of its annual consumption will not increase 50-55 thousand tons. In order to determine production, one should assess the total volume of warehouse uranium stocks in the world as a fuel cycle material (metallic uranium, U_3O_8, and uranium hexafluoride), i.e., both warehouse stocks proper and highly enriched uranium which is already showing up in warehouses as a result of the nuclear weapons dismantling in the United States and CIS.

As for the Western warehouse stocks proper without the materials from the nuclear weapons dismantling, here the picture is clear, and a certain discrepancy in the estimates does not affect the outlook. Thus, an expert from the Nucem Company estimated in 1987 (when the reserves began to be used) that warehoused stocks in the Western countries were approximately 135 thousand tons in terms of equivalent natural uranium [8], so provided that a certain portion of it was used up, the figure amounted to 104 t [sic] by early 1992. According to data from [9], warehouse transition stocks amounted to 113 thousand tons in early 1992. The total reserves estimated in Fig. 1 amount to 120-125 thousand tons, so the difference between production and consumption according to data from the *Nuexco* journal was equal to 160 thousand tons by early

1992, but this also includes the necessary operational reserves. Consequently, one may regard this figure as being equal to 105-125 thousand tons. The situation is more difficult with CIS reserves. According to the Supreme Council expert estimates, by early 1993 [10], the reserves amounted to 100-200 thousand tons in terms of equivalent to natural uranium.

The author of article [11] maintains that American arsenals contain approximately 500 t of highly enriched uranium. A similar magnitude of CIS arsenals has not been determined with the same precision and may vary between 500 and 1,100 t (i.e., a total of 1,000 to 1,600 t). The following data have been cited in some publications: "There are approximately 1,400 t of weapons grade uranium in the CIS" [12] and "500 t in the agreement between the Russian Federal Ministry of Nuclear Power Industry and the U.S. Department of Energy is approximately one-third of our reserves" [13]. It was indicated in the source we already mentioned [10] that Russia's highly enriched uranium reserves reach 600 t.

Let us evaluate the total warehouse stocks from another viewpoint--from the total difference between uranium production in the world and its demand by nuclear power plants. According to data in Fig. 2, this difference in 1970-1992 amounted to approximately 485 thousand tons of natural uranium. A retrospective extrapolation of production and demand curves for 1945-1970 tentatively yields 350-400 thousand tons of excess uranium spent for making weapons. If this was the case, the total reserves would amount to 835-885 thousand tons by 1993. Yet there is a different way of assessing this latter part of excess quantity (up to 1970). There are data indicating that between 1938 and 1970, approximately 330 thousand tons of uranium was mined in the West. Allowing for the fact that a nuclear weapons parity between the USSR and the United States was achieved by 1970-1980 and that the annual production volume in the Eastern European countries was equal in 1970 to the total production in the West according to data in [14], one can assume that prior to 1970, production in Eastern Europe amounted to less than one-half of that. In this case, excess production used for warehouse stocks and nuclear weapons would be tentatively equal to 425 thousand tons. Then the quantity of equivalent natural uranium in warehouses and in weapons in the world would amount to 485+425=910 thousand tons by 1993. While approximately 205-225 thousand tons are stored in warehouses in the form of materials, the stocks of weapons grade materials are (835-910)-(205-225)=(630-660) thousand tons in terms of natural uranium. Furthermore, one should keep in mind that the plutonium production process required approximately 250 t of ^{235}U or, in other words, plutonium production required approximately 60,000 t of natural uranium (we are talking about complete burn-up of ^{235}U in this natural uranium equivalent and not the total quantity of uranium used in plutonium production). In addition to plutonium production, considerable quantities of enriched uranium in the world have been used for military vehicles, primarily as fuel for nuclear-powered submarine reactors. One can roughly state that for this purpose, approximately 300 t of highly enriched uranium has been spent in the world for these purposes which is equivalent to 60,000 t of natural uranium. A smaller but similar quantity of uranium was spent for research reactors. A considerable quantity of reserves in the military sector still remains: 480-510 thousand tons in terms of natural uranium. As one can see, these figures are higher than the maximum in the other authors' estimates. Consequently, in analyzing the future market, we shall use the mean value of 1,000 t for the CIS and 500 t for the United States, i.e., 1,500 t, which is equivalent to 330,000 t of natural uranium. Then the total warehouse reserves reach 525-555 thousand tons, and given a market consumption for approximately 25 years, this amounts to 22,000 t/yr (21.8 t of natural uranium are equivalent to direct production of 100 t of highly enriched uranium from it [sic]). (Enrichment process

losses are lower when 90% ^{235}U is diluted to 4.4%, not with natural uranium, but with 1.5% ^{235}U. If this production method is utilized, 1,500 t are equivalent to 410,000 t, so the total reserves are 615-630 thousand tons, i.e., 25,000 t yr during 25 years or 21,000 t/yr during 30 years). Given a demand level of 55,000 t/yr without taking the latter reserve factor into account, 22,000 t would amount to 40% of world market supply. So it may be necessary to extend the weapons-grade material utilization. But no more than to 2030.

It is also necessary to note that highly enriched uranium utilization by world NPPs also requires cooperation and support by all market participants. It is necessary to allocate a considerable quota for such materials in the world, up to 40% of its demand. Predominant use of warehouse stocks and disarmament-generated materials is also consistent with the policy of resource conservation and economic and environmental requirements. So it is patently obvious that such quantities of natural uranium (30-40% of the market demand) should not be mined during 1998-2020.

The signing of a contract between Russian and U.S. companies for sales of 4.4% enriched uranium obtained from 500 t of highly enriched CIS uranium, 10 t in each of the next five years starting with 1994 and 30 t/yr in the next 15 years, and the possibility of gradually selling off Russian and CIS warehouse stocks will completely obviate the need for setting up new production in 1996-2000 and will serve as a disincentive for natural uranium production in the ensuing period.

And finally, the last conclusion of the uranium balance analysis. After getting to the market, even the minimum volume of uranium mining and production in the CIS (15-20%) and the planned small batches of reprocessed fuel (10%), together with warehouse stock utilization (40-50%), mining enterprises in the rest of the world are left with only 25-35% or 15-20 thousand tons of uranium, i.e., the figure is equal to these countries' current production in 1993 or even less. Thus, it is necessary to discuss a joint policy toward scaling back new production both in the CIS and in the world in 2000-2010 rather than its increase after 2000.

Negative impact of dropping uranium prices and lack of market controls. In uranium utilization, we are still far from reaching the limit of resource conservation. It is perfectly obvious that this can be largely attributed to the military phase in the uranium industry history when the time factor rather than the environmental or economic considerations was the most important. Today, however, the need for resource conservation and possible ways of accomplishing it are becoming increasingly apparent, yet this is in conflict with the economic factors which have already evolved for various reasons, primarily due to natural uranium prices. And even though this may sound paradoxical, the low market price not only fails to stimulate but restrains and largely interferes with increasing the uranium utilization degree.

We have already mentioned the need to increase the fuel burn-up in nuclear power plant reactors. In this case, a decrease in the uranium prices serves as the disincentive, yet this is relatively minor since an increase in the NPP fuel burn-up lowers the whole range of outlays for the preceding fuel cycle, not only for natural uranium, but also for the process of uranium isotope enrichment, fuel element and assembly fabrication, etc. Yet the low uranium prices play a direct negative role in production in the cases where uranium is recovered as a byproduct, as, e.g., a byproduct of phosphoric acid production in the United States at two plants of the IMC Fertilizer Company [14, 15].

Comprehensive raw material processing with the maximum recovery, or better still--with recovery of all components--is a technology of the future. And if the price of the ready product made from one of the components decreases so much as to make it unprofitable to mine it, this is not ecologically viable.

We know that the uranium utilization degree at the stage of enriched ^{235}U is low. At most of the enrichment facilities which shape the enrichment services market, i.e., USEC (United States) and the Eurodif plant (France) where obsolete diffusion technology is used, only 60-75% is recovered from natural uranium with a 0.711% ^{235}U content (60% with a 0.3% tailing, and in extreme cases, 75% with a 0.25% tailing). Even at the more economical production facility of the Urenko Company, its concentration in the tailings is also close to 0.25-0.3.

Yet as the price for uranium increases, it becomes profitable to recover the ^{235}U necessary for thermal reactors more fully. At the Russian plants where centrifugal equipment ensures a low cost of production, conditions exist today for saving natural uranium costing $70/kg by recovering ^{235}U to a residual content of 0.06-0.1% in the tailings, i.e., to bring up the uranium utilization degree to 88-92%. This would lower the demand in natural uranium by at least 40-45% and given 0.06% in the tailings--even by 50%.

The excess isotope separation production capacity being freed up in Russia increases the profitability and probability of increasing the ^{235}U recovery fraction. If all Russian plant facilities are activated, the additionally recovered uranium would be equivalent on the world market to 6-9 thousand tons of natural uranium per year, yet the price for this technical uranium would be less than $60/kg.

This will be even more advantageous when the United States develop the laser-assisted isotope separation production facility where the process would be even more economical. Furthermore, this is a realistic way of developing new jobs in the United States for making up for the job losses resulting from the decline in natural uranium production.

Could it be more efficient to set up joint production for tailings reprocessing: a Russian-U.S. plant with Russian centrifuges which are the most advanced in the world and then hire the American workers who are mining unprofitable uranium in the United States?

As we can see, this way, the uranium production can be decreased by at least 40%, regardless of the size of the NPP uranium enrichment demand market, and we can regard this path as realistic starting with 1995, employing Russian production facilities, provided that economical long-term contracts are signed and that starting with 2000-2005, the U.S. laser production technology is utilized.

Yet one should also keep in mind that since the start of uranium production on a commercial scale (between 1938 and 1993), approximately 1.700-1.800 thousand t of natural uranium have been mined in the world (more than 1 million t of which--in the West) and most of it is now stored in the form of tailings with a 0.3% ^{235}U content. These tailings should be gradually returned for reprocessing in order to recover additional ^{235}U which would be equivalent to bringing into production 500-600 thousand tons of natural uranium. Due to these sources alone one would be able to supply all NPPs in the world with fuel for 10 years.

Finally, it is expedient to use non-burnt-up uranium for reprocessing spent fuel and implementing a closed fuel cycle. According to certain data, secondary materials utilization (uranium and plutonium) is economical at natural uranium prices above $9.5/lb of U_3O_8. And if natural uranium prices are higher, more countries would engage in such reprocessing, so it would be possible to meet the demand of 20-25% of the uranium market in the world by reprocessing, thus lowering the demand for mining.

Also, one should not forget the stocks in the form of weapons-grade plutonium whose utilization in the fuel cycle is more likely, but not until 2005-2010. As one can see from the above figures, even after 2010, there will be no need to increase natural uranium mining. Yet it is perfectly obvious that a higher uranium utilization degree and its lower mining volume would reduce waste at all fuel cycle phases which will make it possible to minimize the negative environmental impact and will call for increasing the outlays for scientific research. Consequently, we should promote and stimulate an increase in the natural uranium prices from the short-term market level to the long-term contract market level.

Need for international government control of production and market in the nuclear fuel cycle. In contrast to even some official viewpoints, the author of this article finds justification for the economic rationale of the complaints against low prices contained in the U.S. antidumping case against the CIS which supplies natural uranium. Yet it would illogical to sign an agreement (or contract) which limits the uranium export volume and in reality--would stop it altogether and both objectives of such a measure appear to be even more illogical: protecting uranium producers in the United States and shutting off one country's market from other, randomly selected supplier countries. These measures have not achieved their objective: They did not enhance the market (by mid-1993, the activity level in the short-term market was considerably lower than that noted in mid-1992 [16]) and did not increase prices in the spot market [17]. While the price rose somewhat in the U.S. market, it fell outside the United States. And the victims were not those who caused the drop in prices by selling off warehouse stocks but U.S. and CIS companies which had not sold off the stocks prior to 1991. Finally, since the free short-term market for such a strategic commodity as uranium, unregulated by the state, would lead to an unacceptable collapse of prices, this would harm not only the interest of individual companies but also for the long-term development outlook, and would require not individual steps to protect one given country but multilateral or intergovernmental agreements and nationwide forms of regulating this market. One can hope that Russia and Euratom will conclude an agreement similar to the one concluded between the Euratom and the United States, Canada, and Australia with equitable uranium shipment quotas for the European market, allowing the shipments from warehouse stocks, both military and civilian. A similar antidumping agreement with the United States is also necessary. Yet these agreements must outline efficient and equitable ways of increasing natural uranium prices, primarily for the purpose of improving the environment and then--for stimulating resource conservation. It is necessary to ensure that the prices reflect an increase in the scope of activities necessary to restore the mines, and not only on the surface but within their entire geographic range. A part of the radioactive waste reprocessing and containment costs should be borne not only by the nuclear power plants but also by uranium producers and must be reflected in uranium prices.

Finally, it is not only necessary but also feasible to increase the prices. Given a general decline in the uranium volume per unit of generated electric power, prices for uranium should increase

disproportionately (some of the profit should be retained by the producer as an incentive). A price floor should be set. According to antidumping agreements, it is expected that some of the constraints on uranium trade between the CIS and the United States will be lifted when the price rises to $13/lb of U_3O_8 ($24 kg of uranium), and all constrains will be lifted after reaching $21/lb (i.e., $40/kg of uranium). Although it is unknown how these prices are set, they are the same as the lowest level necessary for accomplishing the objectives described in this article.

We know that according to the findings of various authors, the use of mixed uranium-plutonium fuel (closed cycle) is economical for various regions compared to uranium fuel (open cycle) at a natural uranium price of between $9.5/lb of U_3O_8 ($18/kg U) and $40-60/kg of U_3O_8 ($20-30/lb of U).

We also know that forecasts for laser-assisted isotope separation in the United States indicate that a price of 1 kg of separation activity is at a $40 level, so 1 kg of technical uranium will cost $60-70, i.e., will be competitive at a higher natural uranium price. This is the same as the price floor.

It is important to retain the price incentives for increasing the quality of the mining and production facilities (without increasing the production volume). And one should not forget to mention the priorities in setting the quotas. The first priority is self-sufficiency, i.e., raw material shipments from the supplying enterprises located in the same country with the consumer, at least to the extent of 20-25% of the demand. The second priority is the sale of nuclear munitions materials; given the necessary controls and protection of these reserves, it is necessary to maximize the most reliable method of preventing their military applications and spent nuclear power plant fuel reprocessing. The third priority is selling off excess warehouse stocks and reprocessing the tailings. The fourth priority is to utilize the richest deposits, both from the quality and quantity viewpoints, as sources of the most economical production and the least harmful environmental impact from their development.

If this is the case, the price of up to 20% of the uranium trade volume will not have to be limited in contracts in order to stimulate the uranium mining and production efficiency; this 20% should be provided at free-market prices as is the case today with the short-term uranium market. Yet in contrast to today's situation with quotas, domestic producers as well as the necessary environmental entities will be protected to a certain extent.

Bibliography

1. 1993 Annual Report of the Urangesellschaft Co.

2. Russia's uranium destabilizes the market. *Tribune* (France), 24 Sept 93.

3. A. Koretskiy. Problems remain despite the resumption of assistance programs. *Kommersant-Daily*, 2 Feb 94.

4. B.V. Nikipelov. Nuclear fuel cycle in Russia. Technical policy. Status and Outlook. Report to the RECOND-94 Conference, London.

5. Nuclear Power, Energy and the Environment. Uranium Institute, June 1993.

6. Energetika: tsifry i fakty (Power enginering: Figures and facts). Bulletin of the nuclear power public information center. Moscow: TsNIIatominform, 1993.

7. Ye.O. Adamov, I.Kh. Ganev, V.V. Orlov. Reaching the radioactive equivalence when handling radioactive waste. *Atomnaya energiya* Vol. 73 No. 1, 1992.

8. G. Larf. Uranium market opportunities in Western countries. *Nukem Market Report* No. 4, 1987, pp. 3-6.

9. L. Raytsin. Americal uranium mining industry is happy to reach these agreements. *Yezhenedelnaya obzornaya informatsiya* No. 48. Moscow: TsNIIatominform, 1992.

10. A. Yorysh, Yu. Rogozhin. *Finansovyye izvestiya* No. 11, 1993, pp. 14-20.

11. F. Berkkhoug, A. Dyakov, Kh. Feyveson, *et al.* Separated plutonium utilization. *Nauka i vseobshchaya bezopasnost* Vol. 3 No. 3, 1993.

12. *Moskovskiye novosti* No. 11, 1993.

13. Environmental Sciences. The World After L10: Merging the Environmental Positions of Nongovernmental Organizations, 1993, pp. 73-75.

14. *Nuexco Review*, 1993, No. 302, p. 35.

15. *Nuexco Review*, 1992 Annual report, p. 16.

16. *Nuexco Review*, 1993, p. 299.

17. *Finansovyye izvestiya* No. 56, 1993.

Operating Experience of EP-500 1R Ceramic Melter for Liquid High-Level Waste Vitrification

947F0148C Moscow ATOMNAYA ENERGIYA in Russian Vol 76 No 3, Mar 94 pp 183-188

[Article by A.S. Polyakov, G.B. Borisov, N.I. Moiseyenko, All-Russian Scientific Research Institute of Mechanical Engineering Standardization imeni A.A. Bochvar, V.I. Osnovin, Ye.G. Dzekun, G.M. Medvedev, V.A. Beltyukov, S.A. Dubkov, Mayak Production Association, and S.N. Filippov, Scientific Research Institute of Chemical Engineering, Yekaterinburg; UDC 621.365:666.1]

[Text] The highlights of more than two and a half years of operation of the improved EP-500/1R ceramic melter at the Mayak Production Association which reprocesses more than 5,250 m^3 of liquid high-level waste with a specific activity of 5-40 Ci/l produced by reprocessing nuclear fuel from VVER-440 reactors and research installations into phosphate glass are summarized in the article. The nitrite waste reprocessed in the melter has the following chemical and radiochemical composition, in g/l:

Al	12.5-20	Sm	0.03-0.3
Na	22-48.3	Ru	0.03-0.1
Fe	0.5-3	Rh	0.01-0.3
In	0.2-2.5	Pd	0.01-0.1
Cr	0.1-0.5	U	0.75-2.5
Ca	0.3-3	Pu	up to 0.01
La	0.03-2.4	Sulfate-ion	0.3-0.9
Ce	0.03-0.3	Free nitric acid	50-129
Nd	0.03-1	Solid phase concentration	132.8-261

The waste has the following radionuclide concentration, in %:

^{90}Sr	28.5-45.2	^{154}Eu	0.7-1.6	^{144}Ce	2.0-7.9
^{137}Cs	35.5-47	^{145}Pm	1.6-1.8	^{106}Ru	1.5-7.9
^{134}Cs	2.1-6.7				

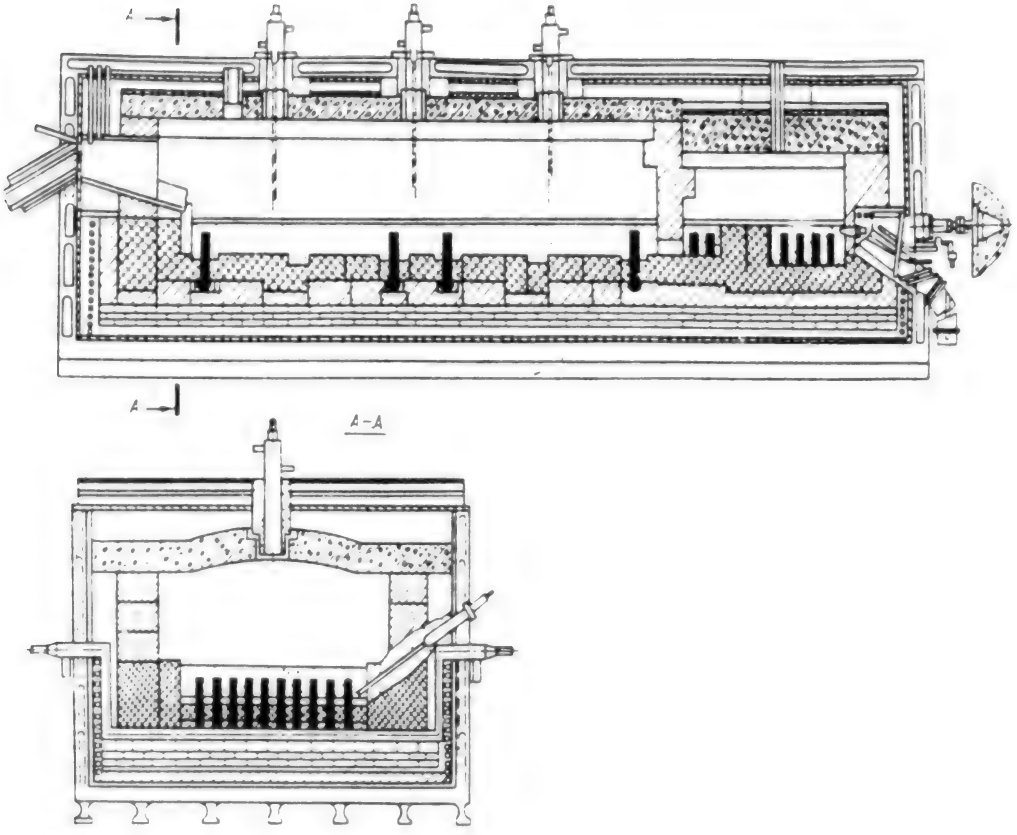

Fig. 1. EP-500 1R ceramic melter (axial and lateral cross-sections).

The principal element of the melter is an electric furnace which is a rectangular pool lined with fused Bacor-33 bricks inside a water-cooled metal housing (Fig. 1). The furnace pool is divided into three zones--melting, transfer, and accumulation. Molybdenum electrode cores encased in water-cooled current leads are built into the floor of each of the furnace zones. Three water-cooled feeders through which the slurry mixed with liquid glass-forming flux (orthophosphoric acid) and ^{106}Ru volatility suppressor (ethylene glycol) is delivered to the glass body surface prior to treatment are installed in the ceiling dome over the melting zone (Fig. 2). Since the start of its operation, 13 batches of fused waste with a volume of up to 120-580 m^3 have been processed; before delivery to the melter, they were mixed for 120 h and their composition was adjusted in order to obtain phosphate glass with the following principal components, in % by mass: 23.09 of sodium oxide, 18.42 of aluminum oxide, 52.21 of phosphorus oxide, and 7.71 total for the oxides of corrosion products, calcium, rare earth elements, zirconium, etc.

As it is produced, the glass melt travels from the foundry zone through the transfer zone to the accumulating zone from where it is periodically dumped into 220-liter containers installed on a stepping conveyor through a discharge unit. According to the existing transport procedure, the containers with cooling glass are packaged into cases with subsequent transfer to a temporary waste storage in the vitrification section. The melter has a capacity of 400±50 l/h of slurry

containing up to 260 g/l of oxides and 100-100 kg/h of vitrified waste. The gas scrubbing system consists of a bubbling condenser, coarse and fine treatment filters, and pyrolusite and absorption columns from where the exhaust gases from the furnace are either pumped or discharged by ejectors into the atmosphere through a stack. The following data on the performance of the principal melter units were accumulated in the course of the melter operation.

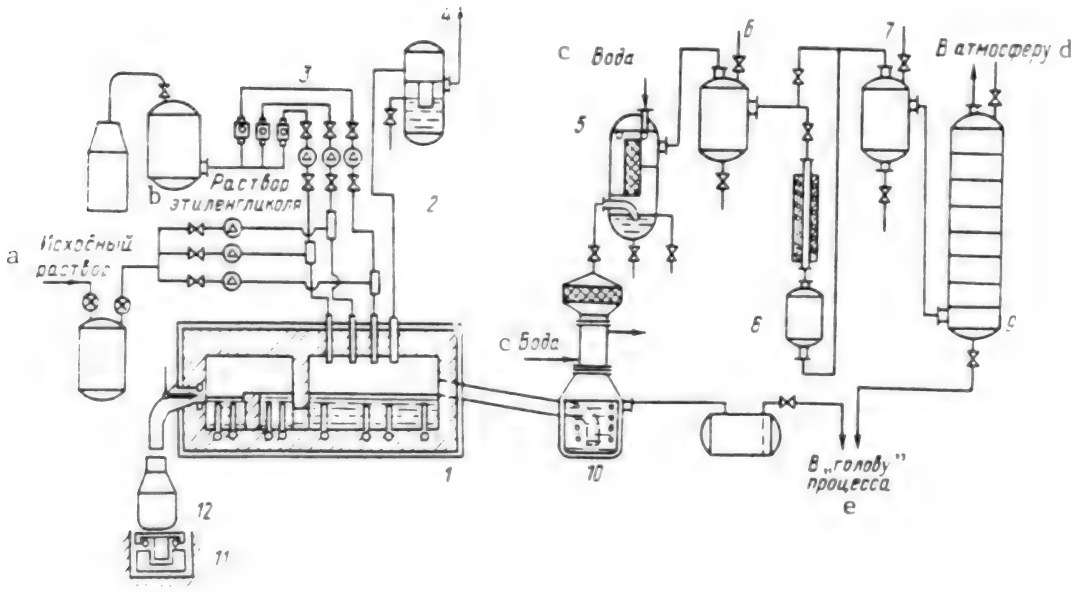

Fig. 2. Block diagram of commercial liquid radioactive waste vitrification furnace: 1--Electric furnace; 2--Mixers; 3--Metering pumps; 4--Hydraulic gate; 5, 6--Coarse and fine processing filters, respectively; 7--Pyrolusite column; 8, 9--Catalytic and absorption columns, respectively; 10--Bubbling condenser; 11--Conveyor; 12--Container; ⋈, ⊗, ⏃--Manual and electric valves and meter; a--Original slurry; b--Ethylene glycol solution; c--Water; d--Into the atmosphere; e--To the "head" of the process.

Electrode assembly. It consists of two sets of electrodes with transverse foundry zone electrode positioning which operate without current transfers with a uniform electric load on the electrodes, thus ensuring the design capacity of 400-450 l/h of slurry as the vitrification process parameters stabilize. With a transition to making lower-melting glass, electric current leaks from the transfer zone to the melting zone which were observed in the earlier operating phases were eliminated. The water cooling system for electrodes and other assemblies operates reliably and ensures continuous delivery of water condensate for cooling individual electrodes and other elements with visual (by the presence of a water jet in the drain funnel) and instrument temperature monitoring (the water temperature at the outlet does not exceed 35°C) and water quality control (with a conductivity of $10^{-4}\Omega^{-1}\cdot cm^{-1}$, pH, etc.). The possibility of tap water ingress into the cooling system is completely ruled out. Studies on a laboratory scale as well as using a pilot EP-100M furnace with a simulator demonstrate that accumulation of a precious metal residue on the melter bottom increases the electric current by 1.5-2 times with all other electric waste vitrification process parameters being equal. Operating experience shows that thus far, no cases of considerable increase in the current in the melter have been observed which indirectly points toward to the absence of noticeable precious metal residue accumulation in the melter.

Glass melt pouring assembly. It consists of two gate and discharging devices. As shown in Fig. 1, the locking and discharging device consists of a water-cooled piston which operates by opening and closing the drain tap in the furnace and a water-cooled drain pipe through which the molten glass enters the containers. A special areaway is designed specifically for accommodating the glass drops and for dissolving the glass in orthophosphoric acid immediately before tapping. During the melter operation, 2,000 glass melt batches were poured into 200-liter containers. During individual vitrification verification periods, the temperature of tapped glass melt reached 1,200°C. This high temperature was probably responsible for burning through the drain pipe in one of the devices which resulted in fracturing the glass jet and glass melt spillage outside the container. After the drain pipe burned through, the glass melt was poured from the furnace through the second gate and discharge device. At present, the glass melt temperature during tapping does not exceed 840-860°C, which creates the conditions for prolonging the safe life of the glass pouring assembly.

Gas scrubbing system. No cases of noticeable gas duct fouling with sublimation products have been observed during the melter operation. The gas scrubbing system ensures a 10^{-5} Ci/l concentration of β-active aerosols (^{137,134}Cs, ^{106}Ru). Today, the volatile cesium, ruthenium, and iodine radionuclide distribution among the gas scrubbing system is still being examined. Nitrous oxide discharges into the environment do not exceed the upper limit of environmental safety standards. Both the operating conditions of the absorption column and the unit of follow-up sanitary purification of the gas flow downstream from the absorption column are being constantly improved because the stringency of sanitary standards for nitrous oxide discharges increases from year to year.

Instrumentation (KIPiA). Before the start of operation, temperature in the melter is monitored by the following instruments:

thermocouples placed under the dome of the furnace and in the gas duct for measuring the exhaust gas temperature;

eight immersible thermocouples in molybdenum housings installed in the melt in the foundry, transfer, and accumulation zones;

thermocouples in the furnace brickwork; and

eight electrode thermocouples placed in the lower sections of the molybdenum rods.

After one year of operation, all immersing thermocouples became disabled for various reasons. Today, the vitrification process temperature is monitored by the flue gas temperature and by the molybdenum electrode temperature. The thermocouples installed in the molybdenum electrodes were calibrated on the basis of the experimental relationships between the thermocouple readings in the molybdenum electrodes and a portable thermocouple periodically immersed into the foundry or accumulation zone melt; this was performed during the melter operation and made it possible eventually to monitor the melt temperature according to the molybdenum electrode thermocouple readings. Glass melt accumulation before tapping was monitored by a glass melt level indicator. At various operating periods, the tapped glass melt was monitored by a gravity device, using visual observation of the glass level in the containers, or by using a gamma-detec-

tor. Operating experience shows that the gamma-detector is the most reliable device for monitoring the tapped glass melt. During the initial furnace operation phases, delays in the glass melt transfer from the foundry to the accumulation zone were observed due to the formation of viscous and solidifying glass. A glass level indicator was introduced for monitoring the glass melt movement in the melter. The use of two glass melt level indicators makes it possible not only to monitor the glass melt movement in the melter but also to determine more reliably the material balance of vitrification using data on the waste charging and glass tapping.

The reason for the development of viscous and crystallizing glass is the presence of suspensions, pearlite, and sand in the solutions which cannot be quantified or characterized. A composition of lower-melting glass with a decreased aluminum oxide concentration was developed in order to decrease the glass viscosity and lower the operating temperature of the glass founding and tapping. A study of the rheological and crystallizing properties of phosphate glass made it possible to demonstrate the possibility of increasing the solubility of suspensions of pearlite, sand, corrosion products, etc., in the glass melt by lowering the aluminum oxide concentration. These glass compositions have been used (Table 1) to process more than 2,900 m^3 of waste. Furnace transition to founding phosphate glass with a lowered aluminum oxide concentration makes it possible to decrease the founding temperature to 950-1000°C and the glass melt tapping temperature to 840-860°C (see Table 1, lines 7-13) thus creating the conditions for extending the melter service life by decreasing corrosion of the molybdenum electrodes, thermocouple casings, and glass level indicators. This decrease in corrosion expands the possibility of using commercial high-temperature alloys as materials for instrumentation sensors, e.g., nickel- and chromium-based alloys.

A decrease in the glass melt temperature in the accumulation zone helps to decrease considerably the discharge of light radionuclides during the glass pouring into the containers (Table 2).

The stability of waste vitrification in the melter is ensured by maintaining an exhaust temperature in the gas duct of 350-420°C. When founding lower-melting glass (batches 7-13), the process occurs at stable parameters and ensures the design initial solution yield of 400-450 l/h. More than 5,200 m^3 of liquid waste has been processed in the melter by 10 Aug 93 and more than 983 tons of phosphate glass with a total β-activity of $136.6 \cdot 10^6$ Ci has been produced and packaged into 2,006 containers and 668 cases, respectively, which were shipped for storage.

Today, waste reprocessing continues, and the melter service life is accruing. Work is underway on justifying the addition of the optimum quantity of waste into the vitrification process with a high concentration of corrosive additives, e.g., iron, nickel, and sulfur.

Thus, the operating experience of the EP-500/1R ceramic melter which handles high level waste and whose production indicators have no counterparts is continuing. A similar melter with a complex design and an output of 170 l/h is still in the development stages in the United States; its operation will be supported by additional heating with the help of electrical resistance heaters located under the roof.

Table 1. Waste processing dynamics and certain vitrification parameters in EP-500/1R melter

Batch No	Batch processing duration, days	Processed batch volume, m	Mean output, l/h	Gas duct temperature, °C	Process temperature range in the zone, °C		Amount of glass tapped, kg	Total glass activity, 10^{7} Ci	Principal glass components, % by mass			
					Foaming	Accumulation			Sodium oxide	Aluminum oxide	Phosphorus oxide	Some of oxides of corrosion products, rare earth elements, etc
1	24	461	289	480 595	1,015 1,135	1,020 1,110	91,831	14,400				
2	58	184	189	500 523	955 1,025	1,010 1,050	61,261	11,052				
3	15	121	409	430	365	1,010	22,338	2,060				
4	54	166	174	495 562	990 1,120	1,000 1,175	64,129	8,841	21 09	18 42	52 21	7 71
5	51	111	106	502 541	1,050 1,130	1,170 1,185	69,951	15,171				
6	29	436	198	515 552	1,080 1,120	985 1,220	79,541	10,113				
7	65	489	402	432 485	1,040 1,060	1,015 1,020	106,327	8,367				
8	14	459	413	432	938	840	85,781	11,114				
9	51	511	450	340	950	860	106,801	17,211				
10	24	261	415	356 430	911 975	840 885	50,500	7,657	25 55	14 33	53 23	7 92
11	19	186	157	345 410	935 1,012	845 881	31,500	10,028				
12	6	41	154	353 400	970 1,000	850 917	11,000	6,556				
13	1	180	421	365 420	950 970	858 910	1 ,500	17,230				
Total	377	5,252	Total processing duration as of 10 Aug 93 2 years and 2 months				981,053	136 7				

Table 2. Concentration of β-active radionuclides at the inlet of the glass pouring gas scrubbing system

Sampling Date	Tapped Glass Temperature, °C	Volumetric Activity of β-Aerosols, 10^{-9} Ci/l
6 Jun 92	1.070	170
24-27 Jul 92	940	44
21-23 Sep 92	840	1.3

Principles of Dose Rate Sensor Placement Around Nuclear Power Plants

947F0148D Moscow ATOMNAYA ENERGIYA in Russian Vol 76 No 3, Mar 94 pp 188-193

[Article by A.P. Yelokhin, All-Russian Scientific Research Institute of Nuclear Power Plants; UDC 539.18]

[Text] The impact of nuclear power plant accidents involving radioactive substance discharges into the atmosphere may be assessed both analytically and by using instruments. The analytical method is based on a software package which calculates the transport of radioactive substances in the atmosphere and the resulting contamination of the environment while the instrumental methods are based on a combination of exposure dose rate sensors of an automatic radiation environment monitoring system (ASKRO) positioned at the monitoring spots at the work site, in the exclusion zone, and in the low-population zone. Demographic, economic, and environmental requirements are imposed on the location of observation stations in the exclusion zone and low-population zone. The demographic requirements are determined by the population density criterion: the monitoring station is set up at an inhabited locality with at least 5.000 residents [1]. The economic requirements are reduced to limiting their number which is due to the high cost of communication lines, equipment (transducers, data receiving and transmitting devices, and microcomputer systems), personnel salaries, expenditures for social purposes, etc. The environmental requirements amount to ensuring highly detailed information about the surrounding environment pollution level for any discharge direction which can be achieved by increasing the number of monitoring stations at the work site and in the exclusion zone.

The resulting contradictions can be resolved if the monitoring stations are positioned along the exclusion zone perimeter. Then given any wind direction, the exposure dose sensors of the automatic radiation environment monitoring system stations will be capable of detecting γ-radiation of the discharge plume or cloud spreading in the wind direction. In this case, the number of monitoring stations is found by the following method. It is assumed that the impurities are being scattered at an altitude of h_{ef} under the worst weather conditions which are usually assumed to be the F-type stability category from the Pasquill-Gifford stability model class [2]. This stability class is characterized by considerable wind-generated transport and a weak transverse discharge plume diffusion. An exposure dose rate equal to the maximum safe dose for group B or $2.3 \cdot 10^{-3}$ mSv/h is selected at a distance of $R \leq 3$ km on the underlying surface assuming that this dose rate is created by the discharge plume spreading in a given direction at a selected point. The dose rate distribution in the direction perpendicular to the radius is calculated on the underlying surface assuming that the maximum safe dose is realized at the distribution peak, i.e., along the radius of the zone boundary. The resulting distribution is used to find the distance at which the dose rate is equal to the sensor sensitivity threshold of $(\dot{D}_\gamma)_{min} \sim 0.1$ mSv/h. If this distance is equal to δ, the necessary number of sensors is determined by the integer of the ratio of

$N_n = [2\pi R/2\delta] = [\pi R/\delta]$ while the sufficient number is greater by a unity, i.e., $N_s = N_t + 1$. For the *F*-stability class, N_t = 22-24. For a different stability class (e.g., A) when the transport rate is low but the impurity diffusion is considerable and other discharge parameters remain unchanged (rate and isotope composition, N_n = 14-15 [3].

Thus, the least number of sensors positioned in the exclusion zone which record the discharge plume at any wind direction for the *F*-stability class or higher is 23-25. We should note that the above monitoring station placement principle is expedient for this zone only in the case where the substances are discharged from the ventilation duct of the nuclear power plant in nominal or emergency conditions. In this case, the most important discharge parameters are the initial temperature and pressure of the jet T_0 and P_0, dose rate P_d, and the isotope composition of the impurities or the spectral composition of γ-radiation which may be measured by special sensors or a combination of sensors installed in the mouth of the ventilation duct. A different situation develops as a result of an unauthorized discharge of impurities in the form of an overheated gas jet from vents, valves, vessel leaks, or torn holes or slots developing as a result of explosion or rupture of reservoirs exposed to high pressures and high temperatures. In this case, it is almost impossible to determine experimentally either the parameters of the jet ejected from the holes or the volumetric activity of the impurities, nor is it possible to determine their radiation characteristics since we don't know either the spectrum or the mean energy of γ-radiation and, in the final analysis, it is impossible to determine the scale of environmental pollution and to assess the ecological impact of contamination since such emergencies are extremely rare and cannot be predicted. Yet the development of versatile equipment which could be used for measuring the above parameters and characteristics in any situation is an almost impossible task and, moreover, may result in sharply increasing the cost of nuclear power plants. Nevertheless, in the case of a substantial surge-like transient impurity discharge through the openings, radioactive contamination of the environment can be assessed by using the readings of the process sensors installed in the vessels which determine the medium temperature and pressure as well as the automatic radiation environment monitoring system sensor readings which determine the exposure dose rate from the cloud formed as a result of the discharge. In this case, neither the work site nor the exclusion zone sensors must be arranged in any specific pattern which requires that the distance from the likely radioactive danger source, i.e., nuclear power plants, to any sensor be strictly different. To confirm this, it would suffice to consider the general equation for the dose rate at points $P_{ijk} = P(x_i, y_j, z_k)$ located on the underlying surface from a bulk source (cloud) with the following volumetric activity distribution in the cloud $q(x, y, z)$:

$$\dot{D}_{ijk} = \dot{D}(x_i, y_j, z_k) = \int_{E_{min}}^{E_{max}} \alpha(E)\,\mu_a(E)\,\varphi(E)\,E \int_V q(x, y, z)\,(B(E, R)/R^2)\exp[-\mu(E)R]\,dv\,dE, \quad (1)$$

where $\alpha(E)$ is the dependence of the detector sensitivity on the γ-radiation energy of impurities in the cloud; $\mu_a(E)$ and $\mu(E)$ are the true absorptivity and linear attenuation of γ-radiation in the air, respectively; $B(E, R) = 1 - a(E)\mu R\exp[b(E)\mu R]$ is the accumulation factor; $a(E)$ and $b(E)$ are known energy functions [4]; $\phi(E)$ is the unknown differential impurity γ-radiation spectrum; x, y, z are the current coordinates; x_i, y_j, z_k are the coordinates of the automatic radiation environment monitoring system sensors; and

$$R = \sqrt{(x - x_i)^2 + (y - y_j)^2 + (z - z_k)^2}.$$

Assuming that the discharge cloud is short in duration, one can ignore its displacement relative to the symmetry axis. The short duration requirement significantly simplifies the method of assessing the cloud exposure dose rate whereas assessment of the dose rate in a dynamic propagation case calls for taking into account not only its deformation during the transport process but also the atmospheric weather factors, the underlying surface roughness, and its contamination degree which considerably complicates the evaluation and lowers the confidence of sensor readings due to their likely radioactive contamination.

Thus, the coordinates of the cloud center of mass can be determined as follows:

$$x_0 = \int_V xq(x, y, z)\, dv/Q_V;\ y_0 = \int_V yq(x, y, z)\, dv/Q_V;\ z_0 = \int_V zq(x, y, z)\, dv/Q_V;$$

$$Q_V = \int_V q(x, y, z)\, dv.$$

Assuming that the distance $R_{ijk} = \sqrt{(x_0 - x_i)^2 + (y_0 - y_j)^2 + (z_0 - z_k)^2}$ from the center of mass to any automatic radiation environment monitoring system station is much greater than the characteristic cloud dimension, we can represent the volumetric activity $q(x, y, z)$ in the following form

$$q(x, y, z) = Q_V \delta(x - x_0)\, \delta(y - y_0)\, \delta(z - z_0), \tag{2}$$

where $\delta(x)$ is the delta-function.

After integration of a volume with $q(x, y, z)$ from expression (2) in expression (1), we obtain

$$\dot{D}(R_{ijk}) = Q_V \int_{E_{min}}^{E_{max}} \alpha(E)\, \mu_a(E)\, (B(E, R_{ijk})/R_{ijk}^2) \exp[-\mu(E) R_{ijk}]\, \varphi(E)\, E\, dE, \tag{3}$$

where $i = 1, 2, \ldots, N_1$; N_1 is the sufficient number of monitoring stations. Equation (3) for $\phi(E)$ is a first-kind Fredholm equation which belongs to a class of incorrect problems for a given sensor measurement error. A nontrivial solution of equation (3) is possible if $R_{ijk} \equiv R_i$:

$$R_i \neq R_{i+1} \neq R_{i+2} \neq \ldots \neq R_{N_1}; \tag{4}$$

Equation (3) is solved by substitution $\phi(E)$ with a group spectrum, by approximating the integral with a finite sum, or, consequently, by a system of linear algebraic equations, i.e., a system of

$$\hat{\mathbf{A}}\, \vec{\varphi} = \vec{\mathbf{D}}, \tag{5}$$

where the $\hat{A}$ operator is an $N_1 \times M$ matrix ($N_1 \gg M$) with a matrix element equal to

$$a_{i,j} = \alpha(E_j)\, \mu_a(E_j) \{1 + a(E_j)\, \mu(E_j)\, R_i \exp[b(E_j)\, \mu(E_j)\, R_i]\} \exp[-\mu(E_j)\, R_i]\, E_j \Delta E;$$

$\vec{\phi}$ is the vector of the unknown solution with the components of ϕ_j, $j = 1, 2, \ldots, M$; **D** is a given vector of measurement results with the components of $D_i = \dot{D}(R_i)R_i^2/Q_\gamma$, $i = 1, 2, \ldots, N$.

Among available methods of solving the system of linear algebraic equations, the most popular are the regularization methods [5-6] and iterative regularization methods [7] in which the unknown solution is found by taking into account the error on both the right side of equation (5) and in the operator $\hat{A}$ if such is present (in this problem, this error may be due to the accumulation factor). On the other hand, special methods have been developed for the ionizing radiation spectrometry tasks which are characterized by a rigid requirement of positive solution $\phi_j \geq 0$, where $j = 1, 2, \ldots, M$ and the absence of error in the $\hat{A}$ operator [8-10].

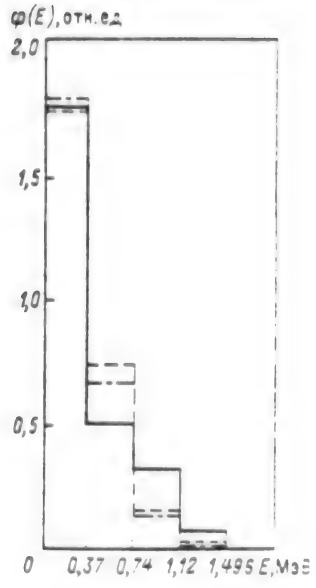

Fig. 1. Bar charts of the original (—, $\bar{E}$ = 0.567 MeV) and reconstructed γ-radiation spectra using methods from [9] (---, $\bar{E}$ = 0.526 MeV) and the regularization method [6] (-•-, E = 0.512 MeV): $\phi(E)$ is in relative units (left).

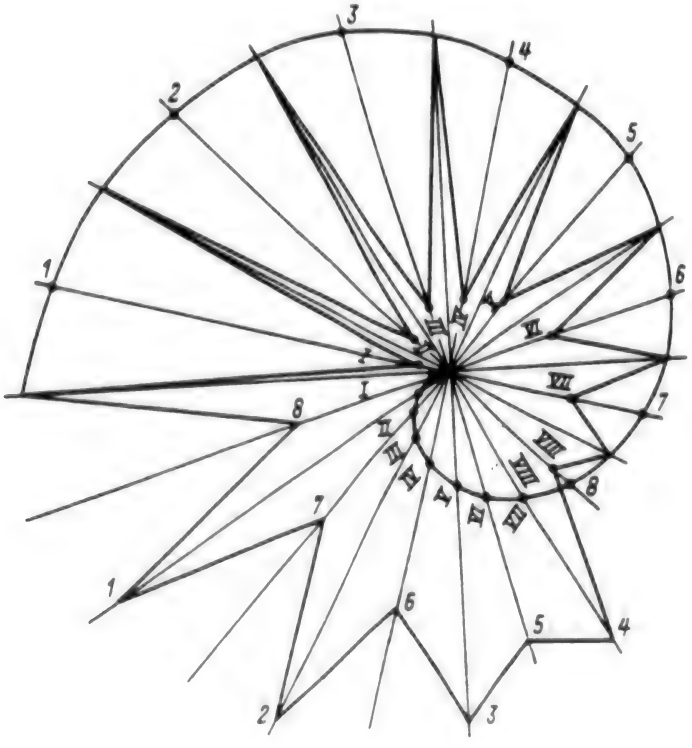

Fig. 2. Likely placement of automatic radiation environment monitoring system monitoring stations in the exclusion zone along the Archimedes spiral (at the intersection of the curve with the rays and in the multiple pointed star at the apices and bases of the rays) (right)

To verify the methods of calculating ϕ_j, we defined the initial spectrum $\phi_{app}(E)$ and then used equation (3) to find $\dot{D}(R_i)$ which was distorted within the real sensor error (30%) after which we solved the inverse problem of determining ϕ_j. One can see from the illustration of the solution of equation (5) shown in Fig. 1 that the original and reconstructed spectra are rather consistent.

while the solution obtained by the matrix inversion (unsatisfactory solution) is shown in the table together with these spectra: $\vec{\phi} = (\hat{A}^*\hat{A})^{-1}\vec{b}$ where $\hat{A}^*$ is the adjoint of the matrix $\hat{A}$; $(\hat{A}^*\hat{A})^{-1}$ is an inverse matrix with $M \times M$ dimensions; $\vec{b} = \hat{A}^*\vec{D}$ is a vector. Condition (4) imposes certain requirements on the placement of monitoring stations around the nuclear power plant: when positioning the monitoring stations (automatic radiation environment monitoring system exposure dose rate sensors), one should avoid axial and central symmetry since otherwise the number of equations (3) or (5) with a differing right side decreases by twofold or fourfold (in the case of axial symmetry) or results in a total degeneration of the system of linear algebraic equations (when the sensors are positioned along the exclusion zone perimeter, i.e., with central symmetry). Furthermore, we have already mentioned that sensor placement along the zone perimeter reliably records the discharge plume or cloud spread for any wind direction. As a result of taking into account these contradicting requirements, the number of monitoring stations R_i must increase with an increase in the azimuth angle measured from any direction (e.g., in the Archimedes spiral). The plots of such curves are shown in Fig. 2; they represent either a smooth curve for which R is a function of angle, $R_i = R_0\theta_i$; $\theta_i = i\Delta\theta$; $i = 1, 2, 3, \ldots, N_\theta$; $\Delta\theta = 2\pi/N_\theta$; $R_0 = 240$-480 mm, or a multipointed star.

Comparison of the original ϕ_{apr} and reconstructed spectra

Energy, MeV	Spectrum $\phi(E_i)$			
	a priori	Calculated by		
		[9]	[6]	Inverse matrix
0.37	1.768	1.784	1.851	-0.088
0.748	0.503	0.731	0.671	0.0
1.1216	0.328	0.149	0.137	-0.802
1.496	$7.358 \cdot 10^{-2}$	$1.56 \cdot 10^{-2}$	$1.447 \cdot 10^{-2}$	$-1.07 \cdot 10$
1.87	$9.6 \cdot 10^{-3}$	$2.28 \cdot 10^{-4}$	$2.13 \cdot 10^{-4}$	2.8434

In determining $\phi(E)$, one can find the mean spectrum energy $\bar{E}$, clarify the total cloud activity, calculate the underlying surface pollution level, and assess the environmental contamination scale as a whole. For a given $\phi(E)$, the mean energy $\bar{E} = \int_E \varphi(E)\, E\, dE / \int_E \varphi(E)\, dE$.

For the $\bar{E}$ value found at the point of the i-th automatic radiation environment monitoring system station, the dose rate can be determined by the following expression [11]:

$$\dot{D} = \dot{D}(R) = 1{,}45 \cdot 10^5 \mu_a(\bar{E})\, \bar{E} \int_V q(x, y, z) \left(B(\bar{E}, R)/R^2\right) \exp\left[-\mu(\bar{E})R\right] dv \quad [\text{мР/ч}]. \tag{6}$$

By using equation (2) and integrating expression (6), we obtain

$$\dot{D}_i = 1{,}45 \cdot 10^5 \mu_a(\bar{E})\, \bar{E}\, Q_V \left(B(\bar{E}, R_i)/R_i^2\right) \exp\left[-\mu(\bar{E})R_i\right].$$

This equation makes it possible to determine $[Q_V]_i$ for each monitoring station:

$$[Q_V]_i = \frac{\dot{D}_i R_i^2 \exp[\mu(\bar{E})R_i] \cdot 100^{-5}}{1.45\,\mu_a(\bar{E})\,\bar{E}\,B\,(\bar{E}, R_i)}, \quad i = 1, 2, \ldots, N_{\text{п}}$$

and its root mean square value of

$$\bar{Q}_V = \sum_{i=1}^{N_{\text{п}}} [Q_V]_i^2 / N_{\text{п}}.$$

The latter value is the total radioactive cloud activity. Thus, together with environmental, economic, and demographic requirements, the requirements for placing the automatic radiation environment monitoring system stations determine the principles of their positioning on the work site, in the exclusion zone, and in the low-population zone around the nuclear power plant.

Bibliography

1. Avtomatizirovannaya sistema kontrolya radiatsionnoy obstanovki v rayone raspolozheniya atomnykh stantsiy (ASKRO) (Computer-aided system for monitoring the radiation environment in the nuclear power plant site region. General specifications). USSR Energy Ministry. VNII-AES. 1987.

2. Effect of the atmosphere's dispersion parameters on the nuclear power plant site selection. Safety publications series No. 50-SG-S.3. Vienna: IAEA. 1982.

3. A.P. Yelokhin, D.F. Rau. Hybrid methods of predicting environmental contamination with the radioactive impurity entering the atmosphere with nuclear power plant discharges. In: Metody rascheta rasprostraneniya radioaktivnykh veshchestv v okruzhayushchey srede i doz oblucheniya naseleniya (Method of analyzing radioactive substrance spread in the environment and population irradiation doses). Moscow: MKhO Interatomenergo, 1992, pp. 91, 283-303.

4. V.P. Mashkovich. Zashchita ot ioniziruyushchikh izlucheniy (Protection from ionizing radiation: A reference). Moscow: Energoatomizdat, 1982, pp. 137-144.

5. A.N. Tikhonov. On robustness of inverse problems. *Doklady Akademii nauk SSSR* Vol. 39 No. 5, 1943, pp. 195-198.

6. A.N. Tikhonov. On solving ill-defined problems and the regularization method. *Doklady Akademii nauk SSSR* Vol. 191 No. 3, 1963, pp. 501-509.

7. V.M. Fridman. Successive approximations method for Fredholm's first-kind differential equations. *Uspekhi matematicheskikh nauk* Vol. 11 No. 1, 1956, pp. 233-234.

8. Scofield N., Proc. Symp. NAS-NS 3017, 1962, p. 108.

9. Su Y. Study of Scintillation Spectrometry Unfolding Methods. *Nucl. Instrum. Meth.*, 1967. Vol. 54. pp. 109-115.

10. Fabian. H.U., Nemsman. U. Determination of the Energy Spectrum of a Gamma-Ray Flash. *Atomkernenergie*. 1970. Bd 16. pp. 143-145.

11. Meteorology and nuclear power. Translated from the English. Leningrad: Gidrometizdat. 1971. 618 pp.

Soil Contamination with Radionuclides in Russia's Residential Areas Due to Chernobyl Nuclear Power Plant Accident

947F0148E Moscow ATOMNAYA ENERGIYA in Russian Vol 76 No 3, Mar 94 pp 209-212

[Article by M.Yu. Orlov, V.P. Snykov, and L.P. Bochkov, Typhoon Scientific Production Association; UDC 539.12.08]

[Text] Today, an assessment of the activity of such long-lived radionuclides as ^{137}Cs, ^{90}Sr, and ^{239,240}Pu is an important tool for determining the habitation and economic activity conditions in Russia's residential areas contaminated as a result of the Chernobyl nuclear power plant accident.

We know that noticeable quantities of these radionuclides entered the natural environment during the nuclear weapons tests in the atmosphere. Consequently, it would be natural today not to focus attention solely on the regions where radioactive contamination differs noticeably from the global pattern. The maximum global fallouts have been observed over the entire globe in the early Sixties, during the peak intensive of atmospheric tests of nuclear weapons.

Estimates show that the density of ^{137}Cs soil contamination (A_s) in European Russia as a result of global radioactive fallout can be regarded today equal to approximately 60 mCi/km^2 [1]. The ratio of independent ^{90}Sr/^{137}Cs yields as a result of fission is equal to 0.47. The ^{90}Sr/^{137}Cs activity ratio virtually does not depend on the time elapsed after the ^{239}Pu nuclear device blast and is equal to 0.39 [2].

Data on the measurements of the ^{90}Sr/^{137}Cs activity ratio measurements in global precipitations over the territory of European Russia are cited in [2]. This ratio averaged over 10 measurements is equal to 0.46±0.05 which is almost the same as the ratio of independent yields.

There is no ^{239,240}Pu in nature since these plutonium isotopes are anthropogenic and enter the natural environment during the explosion of nuclear devices, as a result of emergency nuclear power plant discharges, and with discharges and effluents from spent nuclear fuel reprocessing enterprises where they are formed during the radiation-induced neutron capture by ^{238}U (^{239}Pu) or ^{239}Pu (^{240}Pu) nuclei.

Data on the global fallout of ^{90}Sr, ^{137}Cs, and ^{239,240}Pu averaged for the latitude belts of the northern hemisphere are summarized in the 1977 report by the United Nations Scientific Committee [4]. According to these data, the ^{90}Sr/^{137}Cs activity ratio is equal to 0.625 while allowing for the ^{137}Cs decay, the ^{239,240}Pu/^{137}Cs ratio should be equal to day to approximately 0.015, which is not inconsistent with the results of direct measurements.

The $^{239,240}Pu/^{137}Cs$ activity ratio in global precipitation was measured on several occasions during 1962-1975, and it did not change and remained at a 0.0117±0.0005 level [5]. In so doing, it was assumed that the constancy of the ratio was due to the intake of the corresponding radionuclides due to the Chinese and French atmospheric nuclear blasts. Allowing for the ^{137}Cs decay, this ratio today should be equal to ~0.02.

Allowing for the aforementioned global values of A_{37} as well as the corresponding activity ratios, we can assume the figures of 0.15 and 0.006 Ci/km^2 as the ^{90}Sr and $^{239,240}Pu$ contamination levels (A_{90} and A_{39}), respectively (fivefold values of the corresponding global background contamination) on whose basis one can assert that they are due to the Chernobyl nuclear power plant accident.

Table 1. The number of localities examined and samples measured in Russian territory (as of August 1993)

Oblast	^{137}Cs, number of		^{90}Sr, number of		$^{239,240}Pu$, number of	
	localities	samples	localities	samples	localities	samples
Belgorod	80	530	-	-	-	-
Bryansk	2,194	17,536	490	1,057	97	115
Voronezh	194	1,704	-	-	-	-
Kaluga	601	3,826	92	147	3	13
Kursk	396	1,574	-	-	-	-
Leningrad	71	1,212	13	15	-	-
Lipetsk	116	839	-	-	-	-
Orel	1,407	5,095	21	40	-	-
Ryazan	254	2,437	-	-	-	-
Smolensk	45	226	-	-	-	-
Tambov	79	534	-	-	-	-
Tula	2,366	11,277	58	108	4	9
Total	7,443	45,587	435	805	102	135

One can see from the figures in Table 1 that most attention has been focused on ^{137}Cs contamination since it has been established that the ^{90}Sr or $^{239,240}Pu$ pollution criteria had not been exceeded in any of the residential areas in Russian territory (Table 2, [6]). Indeed, $A_{90} > 3$ Ci/km^2 was not measured in any of the residential areas in Russia. Moreover, no cases of exceeding an A_{39}=0.1 Ci/km^2 have been discovered. In Kaluga and Tula oblasts, A_{90} does not exceed 0.3-0.4 Ci/km^2 in all cases. The maximum A_{90} value was observed in the village of Barsuki in Bryansk oblast--it was equal to approximately 1.3 Ci/km^2. Moreover, in all cases, significant activity of this radionuclide was measured in the areas with a high A_{37}, and not a single locality can be classified as belonging to the, e.g., relocation zone solely due to ^{90}Sr contamination. The highest A_{39} values among the Bryansk oblast localities under study were observed in the town of Klintsy and the village of Velikaya Topal. But even there, A_{39} did not exceed 0.008 Ci/km^2. Individual localities

where noticeable plutonium isotope contamination was also noted were detected in Kaluga and Tula oblasts (up to 0.013 Ci/km^2).

Table 2. Residential area classification criteria

Zone	Criteria
Alienation (Eminent domain)	Relocation and evaluation in 1986
Relocation	A_{37} > 15 Ci/km^2, A_{90} > 3 Ci/km^2 or A_{39} > 0.1 Ci/km^2 Mandatory relocation given A_{37} > 40 Ci/km^2 Average annual effective dose exceeding 5 mSv (0.5 rem) Certain special conditions
Residents with right to relocation	A_{37} from 5 to 15 Ci/km^2 Average annual effective dose exceeding 1 mSv (0.1 rem) Certain other conditions and additional criteria
Right of residents with socioeconomic benefits	A_{37} from 1 to 5 Ci/km^2 Average effective dose not exceeding 1 mSv (0.1 rem) Certain special conditions and additional criteria

In addition to ^{239,240}Pu, ^{238}Pu was detected in all residential areas. The measured ^{238}Pu/^{239,240}Pu activity ratios fall within a 0.2-0.4 range. Calculated estimates for high-power pressure-tube reactor (RBMK) fuel with a corresponding burn-up fraction [7] reach 0.2-0.5 which is quite consistent with the experimental findings.

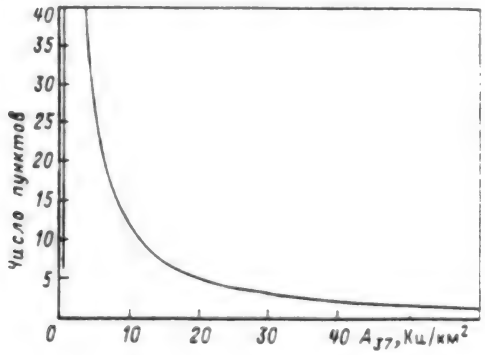

Distribution of the number of inhabited localities based on the mean ^{137}Cs contamination density: Y-axis--Number of localities.

For different estimates, it would be beneficial to examine the empirical dependence $N(A_{Cs})$ where N is the number of inhabited localities with a given pollution level. A description of the corresponding distribution using the least squares method demonstrates that $N(A_{Cs})$ is adequately described by the exponential dependence $N(A_{Cs})dA = (N_0 A_{Cs}^{-2})dA$, where N_0 is the normalization constant. The resulting plot is shown in the figure.

Table 3. Distribution of the number of inhabited localities in Russia by the ^{137}Cs soil contamination level

Oblast	A_{Cs} range, Ci/km^2			
	1-5	5-15	15-40	≥ 40
Belgorod	64	-	-	-
Bryansk	524	283	169	18
Voronezh	57	-	-	-
Kaluga	277	80	-	-
Kursk	155	-	-	-
Leningrad	54	-	-	-
Lipetsk	72	-	-	-
Orel	799	20	-	-
Ryazan	182	-	-	-
Tambov	10	-	-	-
Tula	1,113	170	-	-

The number of inhabited localities classified as belonging to various zones is summarized in Table 3.

Bibliography

1. A.N. Silantyev, I.G. Shkuratova. Obnaruzheniye promyshlennykh zagryazneniy pochvy i atmosfernykh vypadeniy na fone globalnogo zagryazneniya (Detection of industrial soil pollution and atmospheric fallout against the backdrop of global contamination). Leningrad: Gidrometeoizdat, 1983, 136 pp.

2. N.G. Gusev *et al.* Radiatsionnyye kharakteristiki productov deleniya (Radiation characteristics of fission products: A reference). Moscow: Atomizdat, 1974, 224 pp.

3. A.N. Silantyev, I.G. Shkuratova, R.N. Khatskevich. ^{137}Cs and ^{90}Sr in the soil of central regions of European Russia. *Trudy IEM* No. 7 (76) 1977, pp. 120-126.

4. Ionizing radiation sources and effect. U.N. Scientific Committee on the Effect of Atomic Radiation. 1977 General Assembly Report. Vol. 1. New York: United Nations, 1978, 382 pp.

5. Transuranium elements in the environment. Translated from the English. Edited by W. Hanson. Moscow: Energoatomizdat, 1985, 344 pp.

6. Russian Federation Law of "Social protection of citizens exposed to radiation as a result of the Chernobyl Nuclear Power Plant catastrophe." *Vedomosti Syezda narodnykh deputatov RSFSR i VS RSFSR* No. 21, 1991, p. 699.

7. T.S. Zaritskaya, A.K. Kruglov, A.P. Rudik. Transuranium nuclide production during comprehensive utilization of water-moderated water-cooled power reactors and high-power pressure-tube reactors. *Atomnaya energiya* Vol. 46 No. 3, 1979, pp. 183-185.

In-Pile Thermocouple Installation Quality in Water-Moderated Water-Cooled Reactor Tubes

947F0149A Moscow ATOMNAYA ENERGIYA in Russian Vol 76 No 3, Mar 94 pp 227-229

[Article by A.S. Timonin and S.A. Tsymbalov, Nuclear Reactor Institute at the "Kurchatov Institute" Research Center; UDC 621.039]

[Text] *In-situ* coolant temperature monitoring is the necessary condition for economical and safe operation of modern nuclear power plants (YaEU) [1]. In water-cooled water-moderated (VVER) reactors, the fuel element assembly (TVS) coolant outlet temperature is measured by chromium-nickel alloy-alumel cable thermocouples positioned in special protective temperature monitoring channels [2, 3]. As they outlive their useful life, the thermocouples are replaced. This replacement calls for monitoring the insertion of the end of the thermocouple cable with the "hot" junction into the tip of the temperature monitoring channel since this affects the coolant temperature measurement error. If the thermocouple cable end does not reach the mounting seat or is not inserted fully into the seat during the installation into the tube, the size of the air clearance between it and the tube end increases and, consequently, the thermal resistance of the air clearance increases too, which leads to an increase in the dynamic measurement error [4] as well as the error due to the radiation-induced thermocouple heating [5].

Radiation conditions prevailing during the thermocouple replacement complicate direct assessment of their insertion into the channels. A method of indirect evaluation of the thermocouple insertion which is based on analyzing their signal amplitude after heating by an electric current pulse applied to the thermocouple wire is described below. In this case, the assessment of the thermocouple insertion into the mounting seat at the end of the thermal monitoring channel is reduced to evaluating the thermal resistance of the clearance between it and the tip.

The method of applying current to thermocouples has been known and used for various purposes: for testing the electric resistance between the thermocouple wires [6] and between the cable electrodes and sheath [6], for facilitating the extraction of jammed thermocouples [7] and for measuring the thermal response time [8, 9].

Let us consider a model of the thermocouple in the temperature monitoring channel which makes it possible to describe the response of the thermocouple partially inserted into the channel mounting seat to its heating by the current applied to the thermocouple wires.

In order to consider this thermocouple response, it would be sufficient to consider a system of two thermal balanced equations [10] for its cable in the area of the hot junction and thermal monitoring channel end:

$$\rho_1 V_1 c_1 (dT_1/dt) = \alpha_{12} F_{12} (T_2 - T_1) + q_1 V_1;$$

$$\rho_2 V_2 c_2 (dT_2/dt) = \alpha_{23} F_{23} (T_3 - T_2) + \alpha_{12} F_{12} (T_1 - T_2) + q_2 V_2; \quad (1)$$

$$T_1(t = 0) = T_2(t = 0) \equiv T_1(0).$$

where the characters with the subscripts 1 and 2 indicate the thermocouple cable and the temperature monitoring channel tip, respectively; $T_i(t)$ is the temperature averaged over the volume V_i (i=1, 2); $q_i(t)$ is the specific Joule heat release energy; ρ_i and c_i are density and specific heat; $V_{1,2}$ is the volume of the unit of thermocouple cable length and channel tip; F_{23} and F_{12} is the area of the outer surface in the coolant flow and the internal lateral surfaces of the unit length element of the temperature control channel tip; α_{12} is the thermal conductivity of the thermocouple cable contact and channel tip; α_{23} is the coefficient of heat transfer from the channel tip to the coolant; and $T_3(t)$ is the ambient temperature around the thermocouple. It was assumed in deriving formula (1) that the temperature variation factors in the thermocouple and the tip equal to the ratio of the temperature averaged over the thermocouple and tip surface to the temperature averaged over the corresponding volumes are equal to unity. Heat transfers along the thermocouple cable are not taken into account in equation (1). By solving problem (1), we obtain the time dependence of the thermocouple cable temperature in the hot junction region $T_1(t)$:

$$T_1(t) = (\lambda_1 - \lambda_2)^{-1} \{T_1(0)[\lambda_1 \exp(\lambda_2 t) - \lambda_2 \exp(\lambda_1 t)] +$$

$$+ \int_0^t [n_1 q_1(\tau)(\lambda_1 + a_2) + g_2 T_3(\tau) + h_2 q_2(\tau)] \exp[\lambda_1 (t - \tau)] d\tau -$$

$$- \int_0^t [n_1 q_1(\tau)(\lambda_2 + a_2) + g_2 T_3(\tau) + h_2 q_2(\tau)] \exp[\lambda_2 (t - \tau)] d\tau \};$$

$$a_2 = (\alpha_{12} F_{12} + \alpha_{23} F_{23})(\rho_2 V_2 c_2)^{-1}; \; b_2 = \alpha_{12} F_{12} (\rho_1 V_1 c_1)^{-1}; \quad (2)$$

$$s_2 = (\alpha_{12} F_{12})^2 (\rho_1 V_1 c \rho_2 V_2 c_2)^{-1}; \; h_2 = (\alpha_{12} F_{12})(\rho_1 V_1 c \rho_2 c_2)^{-1};$$

$$g_2 = (\alpha_{12} \alpha_{23} F_{12} F_{23})(\rho_1 V_1 c \rho_2 V_2 c_2)^{-1} = \lambda_1 \lambda_2; \; \lambda_1 + \lambda_2 = -(a_2 + b_2);$$

$$n_1 = (\rho_1 c_1)^{-1}; \; \lambda_{1,2} = \{-(a_2 + b_2) \pm [(a_2 - b_2)^2 + 4 s_2]^{0,5}\}/2.$$

Given $T_3(t) = T_1(0) = 0$, $q_2(t) = 0$, and $q_1 = q_1(0) H(t - t_u)$, where t_u is the heating pulse duration; $H(t - t_u)$ is an identity step function, so if $t = t_u$, the solution of equation (2) assumes the form of

$$T_1(t_u) = \frac{q_1(0) n_1}{\lambda_1 \lambda_2} \left(a_2 + \frac{\lambda_2 (\lambda_1 + a_2) \exp(\lambda_1 t_u) - \lambda_1 (\lambda_2 + a_2) \exp(\lambda_2 t_u)}{(\lambda_1 - \lambda_2)} \right). \quad (3)$$

For the TKhA-2076 thermocouple in regular temperature control channels of VVER-440 reactors, one can assume that $\lambda_1 = -a_2$, and $\lambda_2 = -b_2$. This condition is satisfied with sufficient accuracy if $(\alpha_{23}/\alpha_{12}) \gg (r_2/r_1)$. The parameters r_1 and r_2 determine the characteristic thermocouple cable and channel dimensions ($r_i \sim V_i/F_i$, i = 1, 2). In this case, equation (3) is transformed to assume the following form

$$T_1(t_u) = \frac{q_1(0) n_1}{b_2} [1 - \exp(-b_2 t_u)]. \quad (4)$$

Let us consider the case of nominal thermocouple insertion. Given a good cable contact with the channel tip, the thermal resistance of the clearance α_{12}^{-1} decreases. Let $\alpha_{12}^{-1} \to 0$. Then the dynamics of the channel with the thermocouple inserted in it are described by the equation

$$\rho_{12}(V_1 + V_2)\, c_{12}\left(dT_1/dt\right) = a_{23}F_{23}(T_3 - T_1) + q_1V_1, \tag{5}$$

where $T_1(t)$ is the temperature deviation averaged over the channel tip volume with the thermocouple, from steady state to the current pulse; ρ_{12} and c_{12} are the density and specific heat of the "channel tip with thermocouple" structure. Given $T_3(t) = T_1(0) = 0$ and $q_1 = q_1(0)H(t - t_u)$, the solution of equation (5) assumes the following form as formula (4) yet with new values of the parameters b_2 and n_1:

$$b_2 = \frac{a_{23}F_{23}}{\rho_{12}c_{12}(V_1 + V_2)},\quad n_1 = \rho_{12}c_{12}[1 + (V_2/V_1)].$$

Given a pulse duration of $t_u \gg b_2^{-1}$, dependence (4) approaches a constant value equal to

$$T_1(t_u >> b_2^{-1}) = \frac{q_1(0)V_1}{a_{12}F_{12}};\quad T_1(t_u >> b_2^{-1}) = \frac{q_1(0)V_1}{a_{23}F_{23}} \tag{6}$$

for the thermocouple inserted partially and nominally, respectively.

It follows from expression (6) that the amplitude of $T_1(t_u \gg b_2^{-1})$ largely depends on the quality of thermocouple insertion into the tip. Experimental data for two typical installations of the TKhA-2076 (p. 4) into the temperature control channel tip in the protective tubes of the V-213 reactor were obtained during preventive maintenance of the second generating unit at the Rovno NPP in 1990 during the thermocouple heating in one of the temperature control branch pipes when the protective tubes were located in the control well. Nominal thermocouple installation is characterized by the parameter $T_1(t_u \gg b_2^{-1})$ which is smaller than the similar parameter for the thermocouple installed with a depth shortfall in the mounting seat of ~0.2 m. The measurement error makes it possible to predict such a difference.

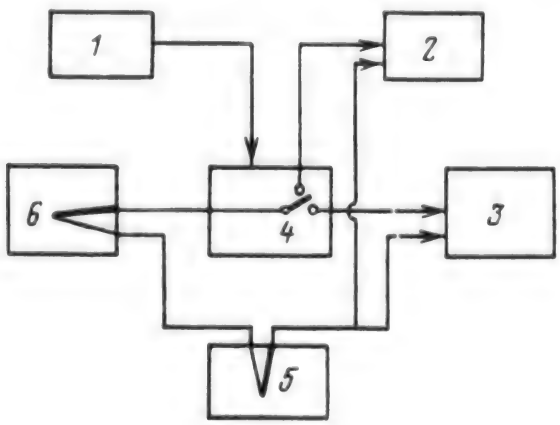

Functional block diagram of the thermocouple heating unit: 1--Control module; 2--Power supply; 3--Thermocouple signal recorder; 4--Circuit switch; 5--Equalization unit; 6--Thermocouple.

A diagram of a unit for electric heating of thermocouples is shown in the figure. The thermocouple wires are heated by pulses shaped by an alternating current power supply source and the control module. Then the control module and the switch are used for switching the heating and thermocouple signal recording cir-

cuits. The recording circuit is a serious connection of the equalization unit, signal recorder, and the thermocouple proper.

A regulating transformer design is selected as the power supply module. A KSP-4 plotter-potentiometer is used as the recorder. An equalization unit designed on the basis of a UPN differential direct voltage amplifier (developed by the Atomic Energy Institute (IAE)) which was used at the nuclear power plant has proven itself reliable and convenient. When taking measurements at the NPP, the heating and recording circuits were switched manually using a stepping switch. The switch design makes it possible to short circuit the recording module input while the thermocouple is being heated.

To eliminate the heating of the "cold" thermocouple wire ends due to heat transfer over the circuits, a nominally installed thermocouple was connected to the unit through a specially designed operational segment with chromium-nickel and alumel buses which were connected to the power cables and equalizing wires. The temperature of the cold junctions was stabilized during the measurements.

The information obtained by analyzing the thermocouple cooling curves after electric heating are also useful for analyzing the temperature measurement error during power operation of nuclear power plants.

Bibliography

1. PBYa RU AS-89 Nuclear power plant reactor safety rules. *Atomnaya energiya* Vol. 69 No. 6, 1990, pp. 409-422.

2. V.Ya. Kotelman, I.P. Kuritnykh. Nuclear power plant temperature measurement devices. *Obzornaya informatsiya TS-6* No. 5, 1986. Moscow: izd. TsNIITEIprib. 20 pp.

3. V.A. Bragin, I.V. Batenin, M.N. Golovanov. Sistemy vnutrireaktornogo kontrolya AES s reaktorami VVER (*In-situ* nuclear power plant monitoring systems for VVER water-moderated water-cooled reactors). Moscow: Energoatomizdat, 1987, 128 pp.

4. A.S. Timonin. Systematic errors in coolant temperature measurements in VVER water-moderated water-cooled reactors (Dynamic errors). *Izmeritelnaya tekhnika* No. 4, 1993, pp. 44-46.

5. A.S. Timonin. Systematic errors in coolant temperature measurements in VVER water-moderated water-cooled reactors (Radiation-induced heating). *Izmeritelnaya tekhnika* No. 5, 1993, pp. 51-53.

6. B.V. Lysikov, V.K. Prozorov, V.V. Vasilyeva, *et al*. Temperaturnyye izmereniya v yadernykh reaktorakh (Temperature measurements in nuclear reactors). Moscow: Atomizdat, 1975, 168 pp.

7. O.M. Fedorov. Upgrading of VVER-440 temperature control system. *Atomnaya energiya* Vol. 67 No. 5, 1989, pp. 354-355.

8. Carroll, R., Shepard, R., Kerlin, T. In-situ Measurement of the Response Time of Sheathed Thermocouples. *Transac. Nucl. Soc.*, 1975, Vol. 21, pp. 427-428.

9. Hashemean, H., Petersen, K., Mitchell, D., et al. In-situ Response Time Testing of Thermocouples. *Inst. Soc. Am. Transac.*, 1990, Vol. 29, No. 4, pp. 97-104.

10. N.A. Yaryshev. Teoreticheskiye osnovy izmereniya nestatsionarnoy temperatury (Theoretical principles of transient temperature measurements). Moscow: Energoatomizdat, Leningrad branch. 1990, 256 pp.

Sulfate-Containing Waste Immobilization in Borosilicate Glass Using Fluoride Additives

947F0149B Moscow ATOMNAYA ENERGIYA in Russian Vol 76 No 3. Mar 94 pp 234-237

[Article by O.K. Karlina. A.V. Ovchinnikov. and M.I. Ozhovan. Radon Scientific Production Association. Moscow: UDC 666.1.055.3:546.226]

[Text] Selection of borosilicate glass as the radioactive waste immobilization matrix is largely justified by the properties of the final vitrified product intended for long-term storage: its high chemical. thermal. and radiation stability [1]. The borosilicate glass structure makes it possible to use it as the matrix for high- and medium-level waste of varying chemical composition. Yet individual waste components. such as sulfate. chloride. and molybdate-containing substances have a limi ed solubility in borosilicate glass [2] which results in a phase separation (stable segregation) during vitrification and a decrease in the vitrified product quality.

Earlier. we proposed vitrification accompanied with recovery of glass-composite materials [3] for sulfate- and chloride-containing waste. In essence. it consisted of mechanical distribution of a melt of vitrophobic components in a glass melt in the form of disperse phase particles with a diameter of up to 200 μm with subsequent mixture cooling until the development of a monolithic glass product with a heterogeneous structure. Thus. the method makes it possible to process waste with a varying chemical composition. including waste-containing vitrophobic components.

Traditional glass. as a rule. does not have an absolutely amorphous structure. Since considerable quantities of alkali and alkali-earth elements and transition series elements are added to radioactive waste-containing glass in addition to the glass base elements. they are usually classified as vitreous materials. Moreover. depending on the chemical composition of vitrified waste areas of microsegregation or crystalline origin are observed in the glass.

This article deals with studying the possibility of processing sulfate-containing waste using the so-called "opacified" glass with a microheterogeneous structure.

We know that fluoride components accelerate the melting of the glass charge and help to intensify vitrification by lowering viscosity and surface tension. Furthermore. fluorides are among the most common and effective opacifying agents used in glass-making. We also know that the opacifying effect is reinforced in the presence of calcium sulfate. The concept of using fluoride additives for vitrifying sulfate-containing waste amounts not only to adding the maximum amount of vitrophobic waste components into borosilicate glass without dispersing the glass melt but also to producing the end product which reliably isolates radionuclides from the environment

The dependence of the degree of sulfate addition to borosilicate glass on the ratio of the sulfate and fluoride ions and the type of the sulfate-containing component was examined in this study.

Chemically pure calcium fluoride (CaF_2) was used as the fluoride-containing raw material. The sulfate-containing waste components were simulated by sodium, calcium, and barium sulfates.

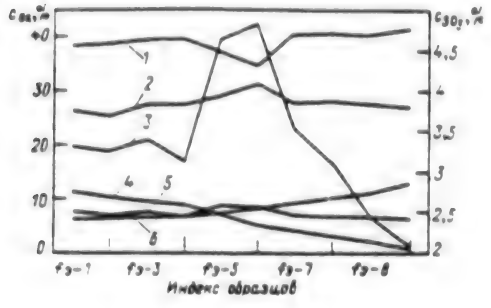

Fig. 1. Chemical composition of glass: 1--SiO_2; 2--CaO; 3--SO_3; 4--F^-; 5--Al_2O_3; 6--Na_2); X-axis--Sample index.

A study was conducted to determine the limits of sulfate phase inclusion into borosilicate glass as a function of the glass composition. A powdered borosilicate frit consisting of chemically pure $CaSO_4$ and chemically pure CaF_2 was mixed in certain ratios. The mixture in alundum crucibles was placed in an electric furnace and exposed to 1,100°C for 1 h. The glass melt was poured off into stainless steel cylindrical molds. The glass samples with a 20 ml diameter and 20 ml height were annealed at 500°C for 0.5 h, then cooled to room temperature under natural conditions. The SO_3 variation in the glass as a function of the base component concentration in the glass under study and the fluoride ion is shown in Fig. 1. One can note an increase in the degree of sulfate integration in the glass with an increase in the fluoride ion and calcium oxide concentration and a decrease in the silicon oxide composition. An increase in the maximum sulfate component concentration led to the sulfate phase precipitation on the glass surface.

Table 1. Chemical composition of charge components

Charge Component	Concentration, % by mass					
	SiO_2	CaO	B_2O_3	Al_2O_3	Fe_2O_3	Other
Quartz sand	98.5	0.3	-	0.4	0.1	0.7
Datolite concentrate	30.7	36.3	17.8	-	2.5	Up to 100
Simulator of liquid waste solids	NaNO$_3$ 69.5	$NaPO_3$ 7.9	$CaCO_3$ 15.2	Mg-$(OH)_2$ 2.0	Fe_2O_3 4.6	NaOH 0.7

Concurrently, experiments to introduce sodium, calcium, and barium sulfates into the charge were carried out to assess the effect of the cation type in the sulfates on the sulfate ion solubility in the glass. The following charge composition was used, in g: 43 of liquid waste solid simulator, 30 of quartz glass, 45 of datolite concentrate (the raw material source composition is summarized in Table 1), 7 of chemically pure Al_2O_3, 25 of CaF_2, and 7.4, 8.9, and 12.1 of chemically pure Na_2SO_4, chemically pure $CaSO_4 \cdot 2H_2O$, and chemically pure $BaSO_4$ respectively. Different calcium and barium sulfate quantities were added due to waste simulation. An analysis of the SO_4^{2-}-ion concentration in the glass indicates a change in its quantity in the samples (content by mass): 2.5% with $CaSO_4$, 2.4% with Na_2SO_4, and 1% with $BaSO_4$. This, in part, is consistent with the premise that the oxide melt tendency toward phase segregation is determined by the extent to which the internal system energy increases when each of the specific types of cation-

oxygen polyhedrons contained in the melt is strained. The greater the cation radius and the smaller its valency, the smaller the bond energy variation resulting from the cation-oxygen polyhedron straining and, likewise, the lower the tendency of the system containing such an oxide toward phase segregation [5].

From the practical viewpoint, we are interested in studying the vitrification conditions of sodium sulfate-containing waste.

Table 2. Charge composition and founding outcome

Index	Component concentration in the charge, g				Sample Appearance	Concentration in glass, % by mass	
	Waste simulator	Quartz sand datolite concentrate Al_2O_3	Na_2SO_4	CaF_2		SO_3	F
S-0	70.6	28.9/35.7	-	-	Uniform translucent glass	Not detected	
S-2	68.6	Same	2	5.5	Opacified glass	1.5	2.0
S-4	66.6	Same	4	11.0	Same	2.2	3.7
S-6	64.6	Same	6	16.6	Same	2.8	5.5
S-8	62.6	Same	8	22.1	Sulfate phase precipitation	3.1	7.1
S-10	60.6	Same	10	25.0	Same	3.3	8.0

The objective of the experiment was to determine the optimum ratio of the fluoride- and sulfate-ions in the charge at which a stable sulfate phase does ont form in the vitrified end product. Quartz sand, datolite concentrate, and simulator of the liquid waste solids (the composition is summarized in Table 1) as well as chemically pure aluminum oxide were used for making the charge. A ^{137}Cs nitrate solution was used as a radioactive tracer (see Table 2).

The charge was ground, mixed in a porcelain pestle, and cured alundum crucibles in a SNOL laboratory electric furnace at 1.100°C for 1 h. The ready glass melt was poured off, annealed, and cooled, as specified for the samples with the compositions shown in Fig. 1.

One can see from the findings in Table 2 that the sulfate phase precipitation commences when the 3% sulfate component concentration in the glass is exceeded. The maximum SO_3 concentration for the compositions used in the presence of a clearly delineated stable segregation was 3.3% whereas when calcium sulfate was used (see Fig. 1), it was up to 4.8% without any traces of stable phase segregation.

According to the IAEA procedure [5], opacified glass samples containing the sulfate component were tested for the ^{137}Cs, Na^+ and SO_4^{2-} leaching stability in distilled water. An analysis of Fig. 2 shows that, as a whole, the leaching rate for both ^{137}Cs and the macrocomponents from S-0 through S-6 samples without any signs of stable segregation does not exceed ~10^{-5} g/(cm^2·day) which meets the IAEA requirements imposed on immobilized radioactive waste.

Compared to Na^+ and SO_4^{2-}, the cesium leaching rate depends less on the sulfate ion concentration in the glass. This indirectly attests to the fact that the sulfate phase is probably concentrated in the microinclusions but the cesium ions are distributed predominantly through the glass phase.

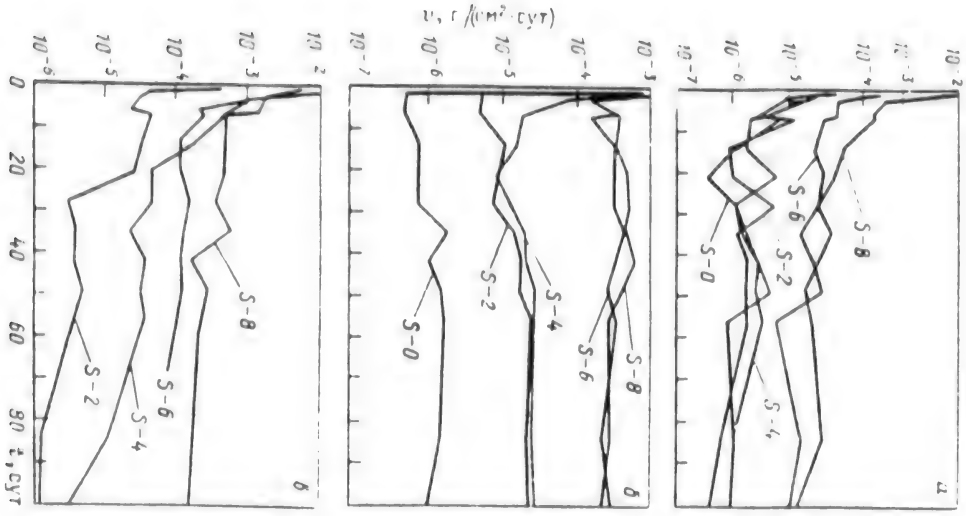

Fig 2. Dependence of the ^{137}Cs (a) Na^+ (b), and SO_4^{2-} (c) leaching rate, in g (cm^2·day) on time, in days, for samples with various sulfate concentrations.

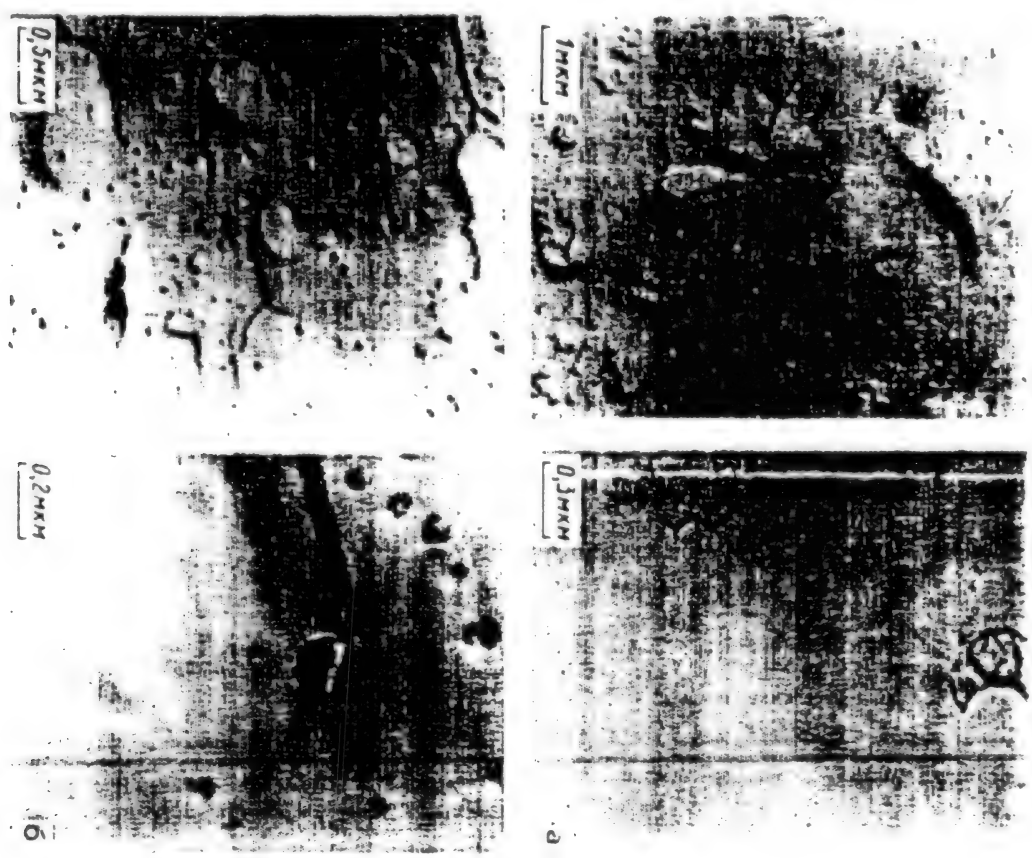

Fig 3. Microphotographs of glass samples containing sodium sulfate (a) and calcium sulfate (b)

According to electron microscope analysis data, the opacified glass samples under study have a microheterogeneous structure with particle sizes varying from 10 to 1,000 nm. Moreover, the presence of both segregation and crystallization irregularities is noted (Fig. 3).

A preliminary analysis of the experiment demonstrates that fluoride-containing additives may be introduced during the vitrification of sulfate-containing waste for resolving the problem of phase incompatibility developing during the integration of this waste in borosilicate glass. The resulting product--opacified glass with a microheterogeneous structure--has an adequate hydrolytic stability for reliable radionuclide immobilization.

By using calcium sulfate as the sulfate-containing component, it is possible to incorporate up to 4.8% of SO_3 in borosilicate glass. We know that sulfate ion inclusion in borosilicate glass is possible against the background of considerable lead oxide concentration [7]. The resulting findings show that the desired effect can be reached by a cheaper method, e.g., by using currently available considerable quantities of fluoride-containing silica gel in chemical industry waste.

Bibliography

1. A.S. Nikiforov, V.V. Kulichenko, M.I. Zhikharev. Obezvrezhivaniye zhidkikh radioaktivnykh otkhodov (Immobilization of liquid nuclear waste). Moscow: Energoatomizdat, 1985, 184 pp.

2. Characteristics of Solidified High-Level Waste Products. *Techn. Rep. Ser.* No. 187. IAEA: Vienna, 1979. 82 pages.

3. O.K. Karlina, M.I. Ozhovan, A.S. Polyakov, *et al.* *Atomnaya energiya* Vol. 72 No. 2, 1992, p. 163.

4. Wolf, M. Chemical Approach to Glass. Amsterdam: Elsevier, 1984, 595 pages.

5. O.V. Mazurin, G.P. Roskova, V.I. Averyanov, T.V. Antropova. Dvukhfaznyye stekla: struktura, svoystva, primeneniye (Two-phase glass: Structure, properties, and applications). Leningrad: Nauka, 1991, 276 pp.

6. Hespe, E. Leach Testing of Immobilized Radioactive Waste Solids. *Atom En Rev*, 1971, Vol. 9, No. 1, pp. 195-207.

7. Shucia, B., Rastogi, R., Sunder Rajan, N.S. In: High Temp. Chem. Proc. Symp., Bombay 28-30 Jan 82, s. l., s.a, pp. 178-183.

Water Leaching Resistance of Irradiated Glass Composite Materials for Medium-Level Waste Immobilization

947F0149C Moscow ATOMNAYA ENERGIYA in Russian Vol 76 No 3. Mar 94 pp 238-240

[Article by O.K. Karlina. and M.B. Kachalov. Radon Scientific Production Association. Moscow:
UDC 661.1.055.3+621.039]

[Text] Radioactive waste is encapsulated in matrices which are chemically inert to the environment (cement. glass. ceramic. etc.) for long-term safe storage [1]. Today. borosilicate glass matrices have the best outlook for this purpose. They are characterized by high radiation and chemical resistance and mechanical strength and adequately confine many waste elements. Yet during glass founding. sulfates form an individual water-soluble phase. One of the methods of neutralizing sulfate-containing waste is dispersing the sulfate phase in the glass melt. The resulting product is a two-phase material in whose glass matrix the distributed sulfate phase inclusions are distributed [2].

One of the principal characteristics of vitrified radioactive waste is its water resistance. High water resistance must be maintained during the entire waste storage period in an irradiation environment due to the radioactive decay of the radionuclides contained in it. The effect of glass composite material irradiation on leaching resistance is examined in this article.

Two types of radiation-induced effects can be identified in the self-irradiation of vitrified waste: electronic--ionization and excitation--and the phenomena of atomic and ionic displacement from the lattice sites.

It was initially assumed that direct atomic displacements make the principal contribution to the defect formation in vitrified glass. During α-decay. the number of direct shifts formed is several times greater than that resulting from any other radiation source. so self-irradiation of vitrified waste containing α-radiators has drawn interest of many researchers [3-6]. It was subsequently demonstrated that ionization processes in vitrified waste also cause considerable defect formation. The importance of ionization processes in defect formation has been established for many silicate systems [7]. including borosilicate glass with radioactive waste [8]. It is demonstrated in this article that compared to electron and heavy ion irradiation. γ-irradiation has the maximum effect on vitrified waste.

Irradiation of glass results in liberation of free oxygen and a change in the glass volume. mechanical properties. and water resistance [9]. It is assumed that these changes have the same origin and correlate. It is also noted in this article that the effect of irradiation on the physical and chemical properties of glass has a threshold nature: these changes in properties have been ob-

served only with an absorbed dose and dose rate higher than the critical level (10^5-10^7 rad and 10^6-10^7 rad h. respectively. for γ-radiation). whereas irradiation affects heterogeneous materials much more than homogeneous. Thus. irradiation of homogeneous and heterogeneous glass led to a change in the material density by 1% and 2%. respectively. The crystalline phase concentration in glass ceramics which are vitreous crystalline materials increased under a γ-irradiation with a 10^5-10^6 R dose [10]. which is much lower than the threshold for homogeneous substances.

An experiment simulating the vitrified sulfate-containing waste storage conditions was staged to check the effect of irradiation on glass composite materials. The glass composite material was produced by the following method. The borosilicate glass frit was mixed in the necessary ratio with powdered sodium sulfate in an alundum crucible with a 0.5-liter volume and placed into an electric furnace preheated to 1.000-1.000°C. The mixture was exposed to this temperature for 1 h until complete melting. then the excess sulfate precipitate was dispersed by a screw impeller in the melt. The melt was poured into molds with a 25-mm diameter and 30-mm height and cooled at a rate of 2 degrees per minute. The resulting composite material was a glass matrix with uniformly distributed round sulfate grains with a 0.1-1-mm size. The glass frit had the following design composition. in % by mass: 47 of SiO_2. 14 of B_2O_3. 21 of Na_2O. 15 of CaO. and 3 of Al_2O_3. The sulfate phase filled 8% of the volume. The samples were irradiated in an RKhM-gamma-20 γ-unit with ^{60}Co radiation sources for 226 h. The dose rate in the irradiation chamber was equal to 0.75 Mrad h. Such a dose rate is 10.000 times greater than the initial dose rate of vitrified waste but does not exceed the critical level for homogeneous glass. A 40-50°C temperature was maintained in the irradiation chamber. The absorbed dose was equal to $1.7 \cdot 10^8$ rad. This dose will be absorbed by vitrified waste with a specific activity of 0.1 Ci/kg during the entire storage life (thousands of years). The waste was leached with distilled water at a 20°C temperature according to the IAEA procedure PerNISO 6961-82. The ratio of the volume water. in cm^3. to the sample surface area. in cm^2. was equal to $V_w/S = 7$. During the first week. water was changed every day. and then weekly during one month. The amount of sodium which passed to the solution was measured by the flame photometry method.

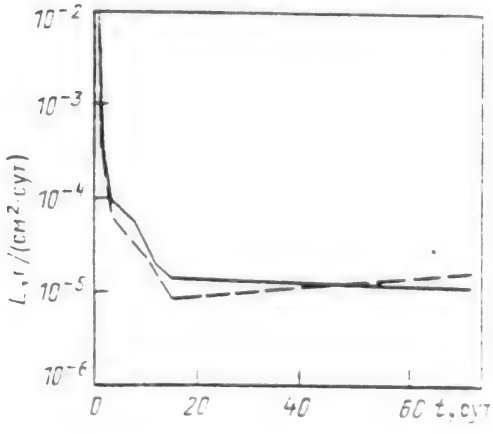

Fig. 1. Irradiated (----) and irradiated (—) glass composite material leaching rate. in g/(cm²·day).

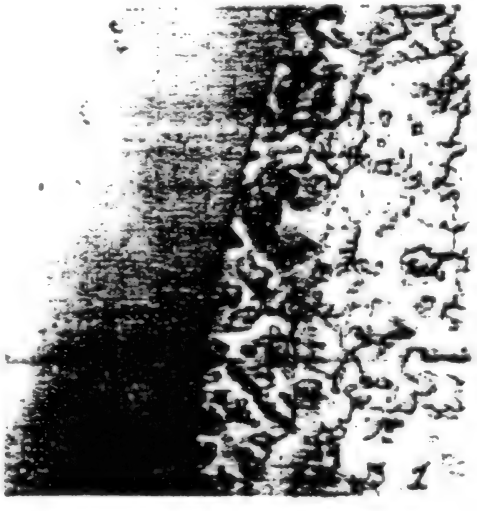

Fig. 2. Sulfate phase (1) and glass matrix (2) of the glass composite material (x 5.8[illegible] magnification).

This test demonstrated that the water resistance of glass composite materials did not deteriorate after irradiation. The test findings are shown in Fig. 1.

Fig. 3. Sulfate phase of unirradiated (x13,200) (a) and irradiated (x21,400) samples (b).

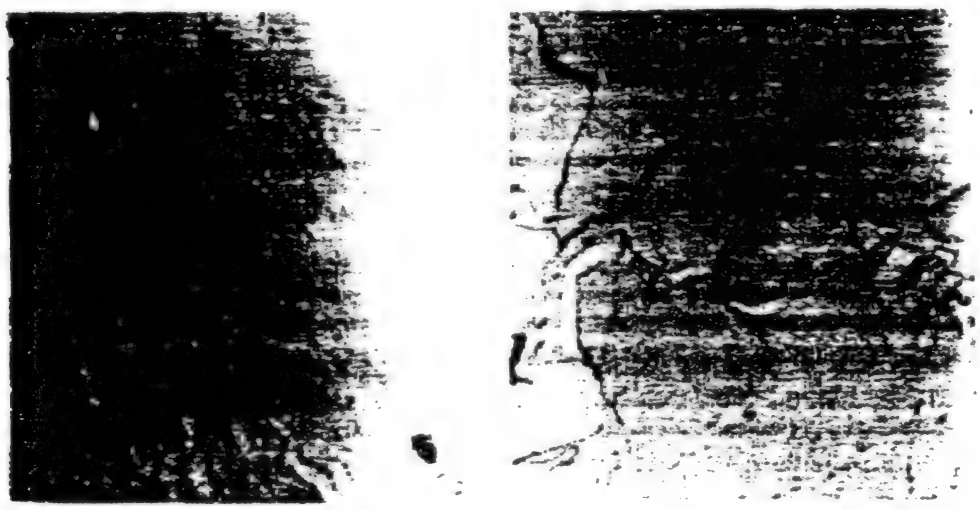

Fig. 4. Glass matrix of unirradiated (x13,200) (a) and irradiated (x13,200) samples (b).

The microstructure of the irradiated and unirradiated glass composite materials was also compared. To this end, carbon replicas were recorded from cleaved irradiated and unirradiated samples and examined under an EMV-100L transmission electron microscope. A microphotograph of the unirradiated glass composite material taken with small magnification is shown in Fig. 2. In this microphotograph, a section with complex relief corresponds to the sulfate base, while the smoother section--to the glass matrix. The microphotographs of the sulfite phase of the irradiated and unirradiated glass composite material are shown in Fig. 3 and those of the glass matrix--in Fig. 4. One can see from the microphotographs that the structure of neither the sulfate phase nor the glass matrix changes after irradiation, and no new characteristic irregularities are discovered.

Thus, the findings of these studies demonstrate that self-irradiation of glass composites due to the radioactive decay of the radionuclides contained in them does not degrade their water leaching resistance during their entire storage life.

Bibliography

1. Stewart, D. Date for Radioactive Waste Management and Nuclear Applications. New York-London: J. Wiley, 1985, 298 pages.

2. O.K. Karlina, M.I. Ozhovan, Ye.M. Timofeyev. USSR Author's certificate No. 1352062. *Byulleten izobreteniy* No. 40, 1988, p. 260.

3. R. Grauer. Kristalline Stoffe zur Verfestigung hochradioactiver Abfalle. *EIR-Bericht* No. 508, 1984, 88 pp.

4. Weber, W., Roberts, F. A Review of Radiation Effects in Solid Nuclear Waste Forms. *Nucl. Technol.*, 1983, Vol. 60, pp. 178-185.

5. Cousens, D., Muhra, S. The Effects of Ionizing Radiation in HLW Glasses. *J. Non-Cryst Solids.*, 1983, Vol. 54, pp. 345-354.

6. Burns, W., Haghes, A., Marples, J. et al. Effects of Radiation Damage and Radiolysis on the Leaching of Vitrified Waste. In: Sci. Bas. Nucl. Waste Manag., New York, 1982, pp. 339-352.

7. Clinard, F., Hobbs, Jr., Hobbs, L. Radiation Effects in Silicate Systems. In: Phys. Radiat. Effects Cryst., 1986, p. 387.

8. De Natale J., Howitt, D. Importance of Ionization Damage to Nuclear Waste Storage in Glass. *Am. Ceram. Soc. Bull.*, 1987, Vol. 66, No. 9, pp. 1393-1396.

9. Weber, W. Radiation Effects in Nuclear Waste Glasses. *Nucl. Instrum Meth Phys Res B.* 1988, Vol. 32, pp. 471-479.

10. S.M. Brekhovskikh, Yu.N. Viktorova, L.M. Landa. Radiatsionnyye effekty v steklakh (Radiation-induced phenomena in glass). Moscow: Energoizdat, 1982, 184 pp.

Fiber Optic Technology in Nuclear Power Industry

947F0149D Moscow ATOMNAYA ENERGIYA in Russian Vol 76 No 3, Mar 94 pp 252-253

[Article by V.B. Anufriyenko and M.N. Arnoldov, Physics and Power Engineering Institute]

[Text] A conference seminar on "Fiber Optic Technology in Nuclear Power Industry and Experiment" was held in November 1993 at the Physics and Power Engineering Institute. It drew participants from seven enterprises.

For the first time in Russia, the outlook for using fiber optic technology in this field of science and engineering was discussed at the seminar.

It was noted in the participants' reports and presentations that fiber optic technology provides a unique opportunity for developing highly reliable automatic process control systems (ASU TP) and primary transducers of various nuclear power plant parameters, both under nominal and emergency operating conditions. This possibility is due primarily to the absolute immunity to electromagnetic interference (including high-power electromagnetic pulses) inherent in fiber optic equipment and its absolute fire and explosion safety. The advantages of fiber optic transducers also include their small mass and geometric dimensions, galvanic isolation, a unified component base for different types of transducers, etc.

Increasing attention is being given to the development of information measurement systems on the basis of fiber optic equipment in world engineering. Back in 1985, various types of fiber optic transducers for measuring more than 60 parameters with high sensitivity and accuracy were developed. Despite the fact that the use of fiber optic equipment in the military and aerospace sector dominates the world market, its utilization in civilian industries is also on the rise (medicine, automobile manufacturing, consumer electronics industry, etc.). An automatic process control system based on fiber optic technology has been commissioned at a petroleum refinery in Japan.

In our country, the development of information measurement systems based on fiber optics is far less advanced. In the nuclear power industry, it is almost nonexistent, although fiber optics have been successfully used since the mid-Seventies for monitoring atomic blast parameters in nuclear engineering.

The obvious potential advantages provided by fiber optic equipment as well as the world experience accumulated through its use in various branches of science and engineering convincingly demonstrate the need to re-evaluate the place of this technology in the nuclear power industry. The seminar was devoted to examining these issues.

Three types of issues which are central for developing fiber optic-based information measurement systems were addressed at the seminar.

The first include the development of transducers important for the nuclear power industry. A report by M.V. Demyanovich (Scientific Research Institute of Instrumentation) described primary transducers of various parameters which may find applications in various branches of engineering, including nuclear engineering: aviation sensors and monitors of the chemical composition of water. Fiber optic technology capabilities are demonstrated by the current amplitude sensor for high-voltage electric networks being developed by the Scientific Research Institute of Instrumentation. Compared to existing current converters, it is approximately 200 times lighter, has a correspondingly lower specific metal content, does not pose a fire hazard since it does not contain oil, etc. In his report, V.V. Ovsyannikov (Physics and Power Engineering Institute) described a pyrometer-type temperature-sensitive element which is characterized by its high accuracy and simple design. Transducers intended for monitoring the vapor phase concentration in the water-based coolant (OKBM) were also discussed. Successful experience has been accumulated in using fiber optic devices for preventing the fuel element mockup burning during the study of critical heat flux in water.

The second range of issues includes the issues of the effect of irradiation in certain fiber optic system components. In his report, O.A. Plaksin (Physics and Power Engineering Institute) presented data on the effect of neutron irradiation on the optical and mechanical properties of single crystal leucosapphire. It is shown that starting with a 10^{18} cm^{-2} fluence, an increase in the luminous flux absorption in the ultraviolet spectral region is observed. As fluence reaches 10^{22} cm^{-2}, absorption bands spread to the visible and infrared spectra. Yet some spectral regions in which the effect of neutron irradiation is not noticeable even at a fluence of 10^{22} cm^{-2} probably remain. We should note that at such a fluence, thermocouples become useless. The mechanical properties of leucosapphire do not undergo noticeable modifications under such conditions yet an increase in its hardness is observed. At the same time, we know that optical quartz fibers are sensitive to irradiation. Keeping in mind that leucosapphire is a stable material under irradiation, it can be regarded as a promising material for use in the nuclear power industry. Since the attainable sapphire fiber length is limited, a transition to quartz fibers and subsequently, to data processing devices, can be made outside the irradiation zone.

The third range of issues dealt with the possibility of manufacturing optical fibers from leucosapphire. It follows from the reports presented by the representatives of the Luch Scientific Production Association (G.I. Goncharov) and Avant Joint Stock Company (Ye.N. Larin) that technical capabilities exist for producing leucosapphire fibers with a 200-300 μm diameter. The bending diameter of such a fiber is approximately equal to 100 fiber diameters, i.e., 20-30 mm. Individual fiber samples with a length of up to 1,000 mm may be manufactured even today. A plant whose design has been completed may be used for large-scale production.

To date, virtually no experience has been accumulated in developing nuclear power plant automatic process control systems on the basis of fiber optic equipment. Yet there is some experience in using optical fibers in automatic control system communication links in one of the reactor plants outside the irradiation zone at the Physics and Power Engineering Institute. This experience demonstrates that the use of optical fibers even on a limited scale results in a sharp decrease

in the number of system operation errors and increases its response speed which is not unexpected for fiber optic technology, yet such an assessment was made for the first time in a reactor unit.

One of the promising trends in fiber optic equipment applications for the nuclear power industry is the development of an information measurement system for determining the parameters of the internal nuclear power plant containment structure under emergency conditions with the primary loop depressurization and oxygen ingress when the requirements imposed on the reliability and fire and explosion safety of the transducers which monitor the evolution of the emergency process are stiffend sharply.

The resolution adopted at the conclusion of the seminar pointed out the good outlook for using fiber optic technology in the nuclear power industry and the need to expand activities in this direction. The decision was also made to hold such seminars regularly once a year to discuss the findings of such activities and coordinate the efforts of the organizations involved.

- END -

Foreign Broadcast Information Service (FBIS) and Joint Publications Research Service (JPRS) publications contain political, military, economic, environmental, and sociological news, commentary, and other information, as well as scientific and technical data and reports. All information has been obtained from foreign radio and television broadcasts, news agency transmissions, newspapers, books, and periodicals. Items generally are processed from the first or best available sources. It should not be inferred that they have been disseminated only in the medium, in the language, or to the area indicated. Items from foreign language sources are translated; those from English-language sources are transcribed. Except for excluding certain diacritics, FBIS renders personal names and place-names in accordance with the romanization systems approved for U.S. Government publications by the U.S. Board of Geographic Names

Headlines, editorial reports, and material enclosed in brackets [ ] are supplied by FBIS/JPRS. Processing indicators such as [Text] or [Excerpts] in the first line of each item indicate how the information was processed from the original. Unfamiliar names rendered phonetically are enclosed in parentheses. Words or names preceded by a question mark and enclosed in parentheses were not clear from the original source but have been supplied as appropriate to the context. Other unattributed parenthetical notes within the body of an item originate with the source. Times within items are as given by the source. Passages in boldface or italics are as published.

SUBSCRIPTION/PROCUREMENT INFORMATION

The FBIS DAILY REPORT contains current news and information and is published Monday through Friday in eight volumes: China, East Europe, Central Eurasia, East Asia, Near East & South Asia, Sub-Saharan Africa, Latin America, and West Europe. Supplements to the DAILY REPORTs may also be available periodically and will be distributed to regular DAILY REPORT subscribers. JPRS publications, which include approximately 50 regional, worldwide, and topical reports, generally contain less time-sensitive information and are published periodically.

Current DAILY REPORTs and JPRS publications are listed in *Government Reports Announcements* issued semimonthly by the National Technical Information Service (NTIS), 5285 Port Royal Road, Springfield, Virginia 22161 and the *Monthly Catalog of U.S. Government Publications* issued by the Superintendent of Documents, U.S. Government Printing Office, Washington, D.C. 20402.

The public may subscribe to either hardcover or microfiche versions of the DAILY REPORTs and JPRS publications through NTIS at the above address or by calling (703) 487-4630. Subscription rates will be provided by NTIS upon request. Subscriptions are available outside the United States from NTIS or appointed foreign dealers. New subscribers should expect a 30-day delay in receipt of the first issue.

U.S. Government offices may obtain subscriptions to the DAILY REPORTs or JPRS publications (hardcover or microfiche) at no charge through their sponsoring organizations. For additional information or assistance, call FBIS, (202) 338-6735,or write to P.O. Box 2604, Washington, D.C. 20013. Department of Defense consumers are required to submit requests through appropriate command validation channels to DIA, RTS-2C, Washington, D.C. 20301. (Telephone: (202) 373-3771, Autovon: 243-3771.)

Back issues or single copies of the DAILY REPORTs and JPRS publications are not available. Both the DAILY REPORTs and the JPRS publications are on file for public reference at the Library of Congress and at many Federal Depository Libraries. Reference copies may also be seen at many public and university libraries throughout the United States.

END OF FICHE DATE FILMED

30 August 1994